

H.-J. FREUND, M. BÄUMER, J. LIBUDA, H. KUHNENBECK, T. RISSE,  
K. AL-SHAMERY, H. HAMANN

Fritz-Haber-Institut der Max-Planck-Gesellschaft,  
Faradayweg 4–6, D-14195 Berlin, Germany

## Metal Aggregates on Oxide Surfaces: Structure and Adsorption

### 1. Introduction

The growth of metals on oxide substrates has been the subject of many studies in the past (e.g. see the review article of Campbell (CAMPBELL 1997) and references cited therein). One of the reasons for the interest in these systems results from the potential they have as model systems for supported metal catalysts, since they facilitate a detailed investigation of the interplay between the structure of such composite systems and their interaction with adsorbates.

There are several examples showing that it is within reach to establish correlations between particle size and electronic properties on the one hand and adsorption behavior or catalytic activity on the other hand (LAMBERT 1997, FREUND 1997-1).

Typical metal support systems are those in which the metal is a transition metal, and the support is, for example, composed of  $\text{SiO}_2$ ,  $\text{Al}_2\text{O}_3$ , or  $\text{MgO}$ . We can produce well-ordered layers of  $\text{MgO}$  (WU 1992 and 1993, HE 1992, HEIDBERG 1993, HENZLER 1993, SCHWENNICKE 1993, TRUONG 1993, VESECKY 1994, ZECCHINA 1996, SCHRÖDER) and  $\text{Al}_2\text{O}_3$  (JAEGER 1991, WUTTIG 1991, JAEGER 1993-1 and -2, LIBUDA 1994-1 and -2, CHEN 1994, WU 1995, WU). The preparation of ordered  $\text{SiO}_2$  layers still gives difficulties (STEMPEL). We have focused our attention until now on the support system  $\text{Al}_2\text{O}_3$ , and, thus in the following, initially the structure and properties of the support (JAEGER 1991, LIBUDA 1994-2) as well as the possibilities of its chemical modification by functionalization (LIBUDA 1996-1) will be considered, and, thereafter, the growth, morphology, electronic and magnetic structure as well as adsorption and reaction behavior of the metal films deposited (LIBUDA 1995, LIBUDA 1996-1 and -2, FREUND 1993, WINKELMANN 1994, WOHLRAB 1996, BERTRAMS 1995, BÄUMER 1995, SANDELL 1995, 1996, 1997 and 1998).

### 2. Structure of a Support

A well-ordered, thin  $\text{Al}_2\text{O}_3$  film can be generated on a (110) surface of a NiAl alloy single-crystal by oxidation and tempering at 900 K (JAEGER 1991, LIBUDA 1994-2). The choice of this system has several advantages. If one tried to produce an  $\text{Al}_2\text{O}_3$  film on an Al substrate, a film would be produced that covers the whole surface, and thus to order this film, the temperature would need to be raised to such an extent that the substrate would melt. In contrast, NiAl has a high melting point of 1638 °C.  $\text{Al}_2\text{O}_3$  is produced on

the surface by oxidation; the freed Ni dissolves in the NiAl bulk through heating, because the thermodynamically most stable phase in the NiAl system is the nickel-rich  $\text{Ni}_3\text{Al}$ . The dissolution of nickel in the bulk can be monitored, for example, by ESR spectroscopy (KATTER 1993). The thickness of the film was determined to be 4–5 Å from angle-dependent X-ray photoelectron spectroscopy (ADAM 1991) and from Auger spectroscopy (ISERN 1989). The stoichiometry of the film corresponds within the limits of experimental error to that of  $\text{Al}_2\text{O}_3$  (JAEGER 1991). Photoelectron spectroscopy and EEL spectroscopy were used to show that the film contains no metallic Ni and no NiO (JAEGER 1991). The film is chemically unreactive, and CO adsorbs on it only at low temperatures (<80 K) (JAEGER 1993-1 and -2), whereas CO binds to the NiAl substrate

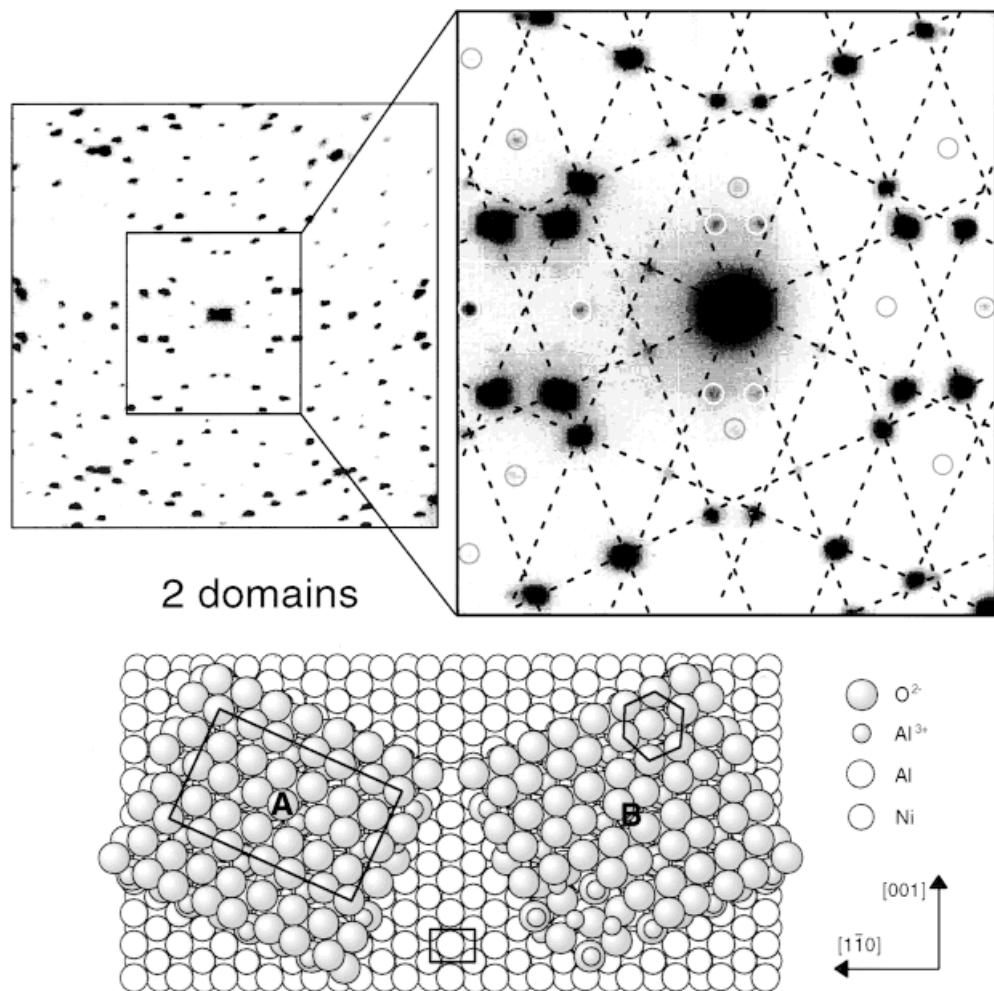


Fig. 1. Top: LEED pattern (85 eV) of the  $\text{Al}_2\text{O}_3/\text{NiAl}(110)$  system with a close up of the region around the (0,0) reflection. The spots that appear in addition to those of the oxide (marked circles) are attributed to double scattering at the substrate and oxide structure. Bottom: Schematic structural model derived from  $\gamma\text{-Al}_2\text{O}_3$ . The rectangular unit cell of the oxide superstructure as determined from the diffraction pattern is marked

up to significantly higher temperatures (GAYLORD 1987, MUNDENAR 1988). Thermal desorption studies confirm that the film formed covers the whole surface of the alloy.

The  $\text{Al}_2\text{O}_3$  film is remarkable in the way it spreads some time over the steps of the substrate like a “carpet”, a phenomenon that is known, for example, for the growth of alkali metal halide films on elemental semiconductors (PFNÜR 1993).

Figure 1 shows the electron diffraction pattern of the film together with a schematic structural model (JAEGER 1991). The LEED picture still shows the reflections of the substrate. Superimposed onto the substrate spots are the reflections derived from a superposition of two domain LEED patterns, as indicated in the diagram. The double diffraction reflections through scattering on the  $\text{Al}_2\text{O}_3$  film and substrate exist but are weak (see Fig. 1) (WUTTIG 1991). The two domain directions A and B are at an angle of  $24^\circ$  with respect to the  $[110]$  direction of the substrate. This twist is forced by the arrangement of the large, nearly rectangular unit cells on the  $(110)$  NiAl surface. The arrangement of the  $\text{Al}_2\text{O}_3$  layer in the  $[110]$  direction is substrate-related and commensurable, in the perpendicular direction, however, incommensurable.

Figure 2 shows an STM image of the domain interface (LIBUDA 1994-2), which has no atomic resolution. Rather the protrusions show a global variation of the electronic structure about the marked unit cells. The STM image was recorded under conditions at which electrons from the oxide layer tunnel to the tip of the scanning tunneling microscope. Since the occupied density of states of the oxide begins at about 4 eV below the Fermi energy of the alloy substrate, high tunneling voltages are required. Therefore, the distance between the tip and the substrate is relatively large, and the lateral resolution is limited. If small tunneling voltages are used, the electrons tunnel mainly from the substrate through the film to the tip. This can be used to reproduce the atomic structure of the NiAl layer immediately underneath the  $\text{Al}_2\text{O}_3$  film.

The thickness of the  $\text{Al}_2\text{O}_3$  film is comparable with two Al-O double layers, as shown schematically in Fig. 3.

The  $\text{Al}_2\text{O}_3$  film is oxygen-terminated, as we know from ion-scattering spectroscopic experiments (WINKELMANN 1994, WOHLRAB 1996, BERTRAMS 1995). Both, the intensity distribution in the electron diffraction pattern and the measurements of the  $\text{Al}_2\text{O}_3$  band structure by angle-resolved photoelectron spectroscopy hint at the formation of hexagonal oxygen layers (JAEGER 1991). Additional evidence for the formation of the

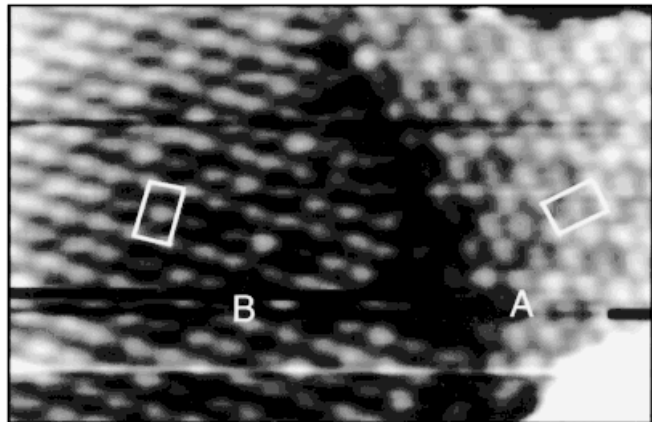


Fig. 2. STM image of the  $\text{Al}_2\text{O}_3/\text{NiAl}(110)$  system (CCT,  $210 \text{ \AA} \times 130 \text{ \AA}$ ,  $-2 \text{ V}$ ,  $0.5 \text{ nA}$ ). The unit cells of the differently oriented domains A and B are indicated

oxide layer is obtained from photoelectron spectra in the region of the Al-2p core electrons (JAEGER 1991). The photoelectron spectroscopic signals of individual layers in the film are assigned in Fig. 3: The sharp doublet arises without doubt from the alloy support; the weak shoulder at about 74 eV must stem from the interlayer region, since it returns strongly in terms of its relative intensity when the spectrum is recorded at grazing electron emission, that is, lower escape depths of the electrons (ADAM 1991); the most intense signal in the photoelectron spectrum stems from the fully oxygen-coordinated Al ions. The nature of the coordination environment (octahedral or tetrahedral) of the Al ions is hard to decipher from this information alone. Complementary information is provided in Fig. 3 (bottom right) from the phonon spectrum of the film (JAEGER 1991), which was recorded by using electron loss spectroscopy. Comparison with the spectra of  $\alpha$ - and  $\gamma$ -Al<sub>2</sub>O<sub>3</sub> leads to the conclusion that the coordination corresponds more to that of  $\gamma$ -Al<sub>2</sub>O<sub>3</sub> than that of  $\alpha$ -Al<sub>2</sub>O<sub>3</sub>. This means that tetrahedrally and octahedrally surrounded Al ions are present.

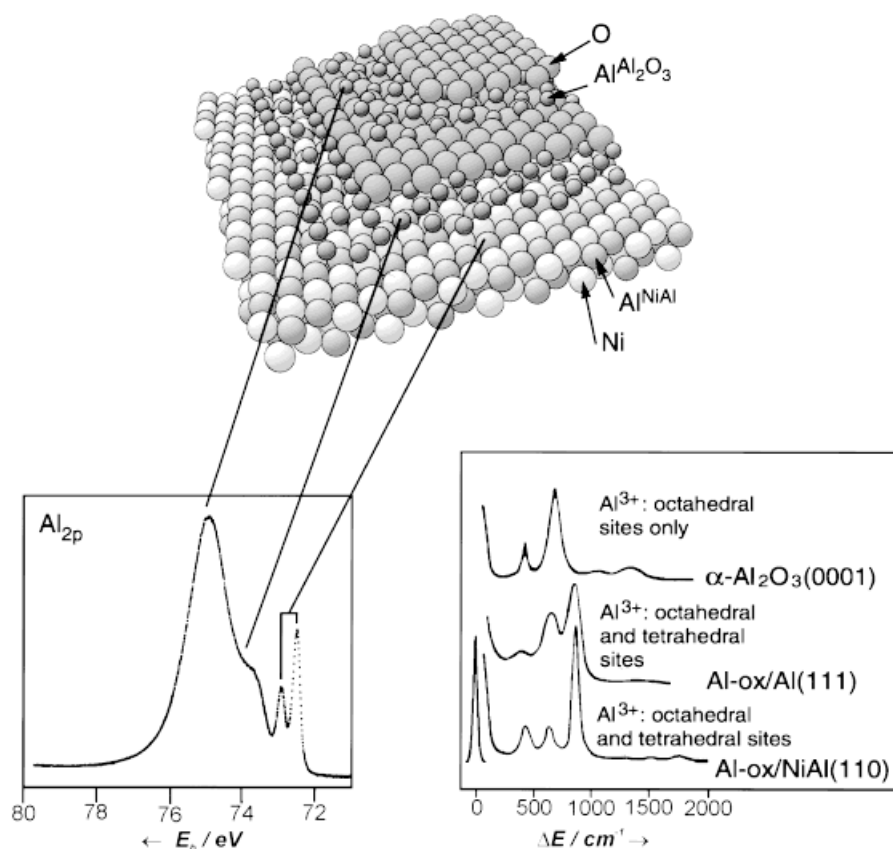


Fig. 3. Top: Schematic model of the Al<sub>2</sub>O<sub>3</sub>/NiAl(110) system. Bottom: High resolution photoelectron spectrum (left hand side,  $h\nu = 150$  eV, perpendicular emission) and high resolution electron energy loss spectrum (right hand side). Substrate, interface, and oxide components are clearly separated in the photoelectron spectrum ( $E_b$  = binding energy). The HREEL spectrum of the Al<sub>2</sub>O<sub>3</sub> film on NiAl(110) is compared to those of Al(ox)/Al and  $\alpha$ -Al<sub>2</sub>O<sub>3</sub> ( $\Delta E$  = energy loss)

We have thus achieved an extensive characterization of the film and established that we are dealing with a well-ordered  $\text{Al}_2\text{O}_3$  film, which is free of hydroxyl groups and which fully covers the surface. Evidently, this film cannot correspond in every way to a bulk single crystal, since in the direction perpendicular to the surface the thickness of a unit cell of  $\gamma\text{-Al}_2\text{O}_3$  or  $\alpha\text{-Al}_2\text{O}_3$  is not achieved. Nevertheless, it appears that in many ways the properties of this film are typical for  $\gamma\text{-Al}_2\text{O}_3$  and the layer thickness has only a limited influence on the observed properties.

The film prepared in this way can now be directly covered with metal, but it can also be chemically modified prior to the introduction of the metal (LIBUDA 1996-1). Thus, it has been possible to study the influence of functional groups on the  $\text{Al}_2\text{O}_3$  surface on the growth and reactivity of thin metal films: Of special significance in this context are hydroxyl groups on the  $\text{Al}_2\text{O}_3$  surfaces, and in the following, the ways in which chemically modified films can be prepared will be discussed briefly (LIBUDA 1996-1, ALMY 1977, PAUL 1986, CHEN 1986, COUSTET 1994, FREDERICK 1991, SCHILDBACH 1993, McDONALD 1965, CHATAIN 1986, BAUER 1958).

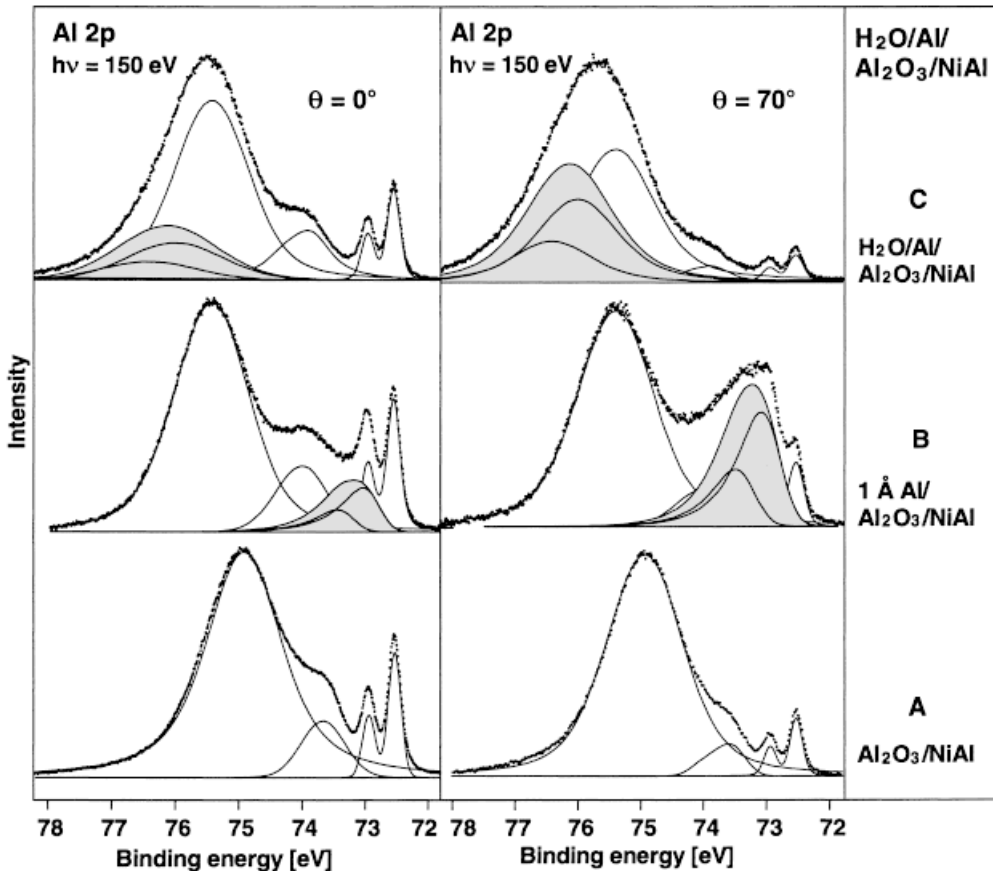


Fig. 4. Al 2p photoemission spectra of the chemically modified  $\text{Al}_2\text{O}_3/\text{NiAl}(110)$  surface ( $h\nu = 150$  eV at grazing ( $70^\circ$ ) and normal emission). A: Clean  $\text{Al}_2\text{O}_3$  film; B: After deposition of 1 Å Al at 300 K; C: After  $\text{H}_2\text{O}$  exposition at 90 K and subsequent warming up to 300 K

The basic concept is the following: Metallic aluminum is adsorbed onto the ordered  $\text{Al}_2\text{O}_3$  film and then the layer thickness can be increased by oxidation with either pure oxygen, or, by oxidation with  $\text{H}_2\text{O}$ , a somewhat thicker hydroxylated aluminum oxide layer is achieved.

This process can be monitored by photoelectron spectroscopy (Fig. 4) (LIBUDA 1997). The bottom spectra (A) are those of the clean  $\text{Al}_2\text{O}_3$  film, on the left hand side obtained by perpendicular electron emission, and on the right hand side by grazing electron emission. Deposition of a part of a monolayer of metallic aluminum leads to the spectra B. From the production and the comparison with different spectra recorded at different angles of emission, it can be seen straight away that Al lies on the surface of the  $\text{Al}_2\text{O}_3$  layer. Notably, in addition to the appearance of new bands, the whole spectrum is shifted to a higher energy range. This is attributed to the fact that depending on the charge polarization in the interfacial layers, potential differences occur through the insulator layer. These differences can also be discussed in terms of band bending (LIBUDA 1996-1) and lead to these shifts. Hydroxylation with water leads to a conversion of the metallic aluminum to the ionic form and to the top spectrum in the series (C). At the same time, the O 1s spectrum indicates the formation of a shoulder, which is typical for the presence of hydroxyl groups. It is not surprising that through this process the order of the surface is changed, though it is by no means fully lost. The concentration of functional groups can be controlled by varying the dosage of aluminum. Evidently, it is conceivable that the formed OH groups can be used to further functionalize the surface.

### 3. Morphology of Metal Deposits

Metals can be deposited on clean and on chemically modified surfaces. Figure 5 shows several examples resulting from metal deposition on a thin alumina film.

Remember that, for the function of catalysts the morphology and structure of the metal deposits is very important, because it determines the activity and selectivity in the chemical process. Different metals exhibit very different growth modes which depend to a large extent on the strength of interaction between the metal and the oxide substrate. This in turn is strongly influenced by the presence of defects, such as steps or domain boundaries or point defects on the substrate. Silver as an example only weakly interacts with alumina and is consequently very mobile at room temperature. It nucleates at steps and forms relatively large but only few aggregates (bottom of Fig. 5). Platinum or cobalt and rhodium, on the other hand, interact more strongly with the oxide substrate, are less mobile and thus form small particles upon deposition at room temperature (top of Fig. 5). Such investigations give direct insight in how the substrate has to be conditioned for a given metal in order to prepare a certain dispersion of metal particles. The adsorption energy  $E_{\text{ads}}$  is described by the classical Young approximation (CHATAIN 1986, BAUER 1958, LIBUDA 1997), for which approximate values are known for the first two interaction energies, but the oxide/metal term is usually not known.

$$E_{\text{ads}} = E_{\text{oxide/gas}} + E_{\text{metal/gas}} - E_{\text{oxide/metal}}. \quad (\text{a})$$

Which growth behaviour is observed at a given temperature depends on  $E_{\text{ads}}$ . If  $E_{\text{ads}} < 0$ , full coverage is attained, that means a layer growth of the Frank-van der Merwe type. If  $E_{\text{ads}} > 0$ , three-dimensional islands are formed (Volmer-Weber growth mode) (LIBUDA 1997). If a layer-by-layer growth is replaced at a known layer thickness by a three-dimensional growth, it is referred to as a Stranski-Krastanov mode. Naturally, the de-

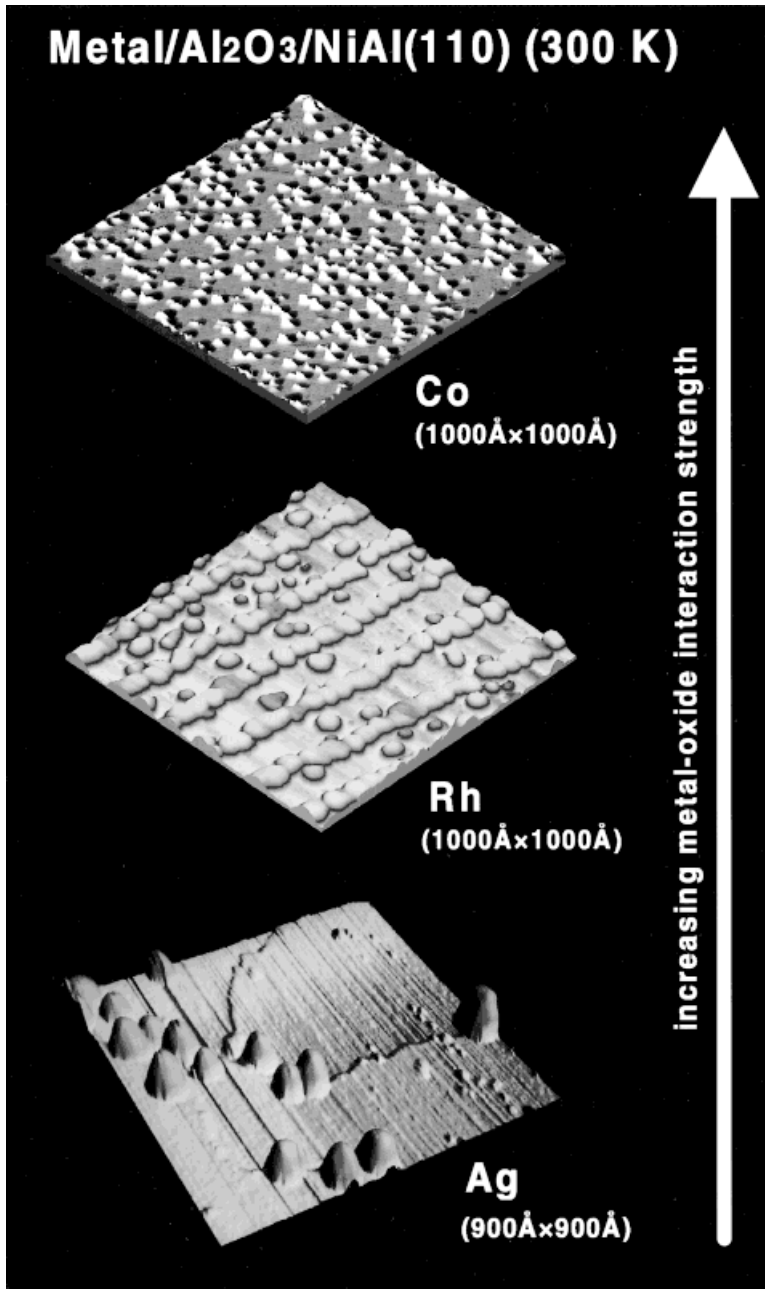


Fig. 5. STM images of Co, Rh and Ag deposited on Al<sub>2</sub>O<sub>3</sub>/NiAl(110) at 300 K

tailed defect structure of the substrate and the introduced particles play an important role for these processes, since the defects of the oxide layer are nucleation centers for the deposited particles, as is apparent from Fig. 5 (middle panel).

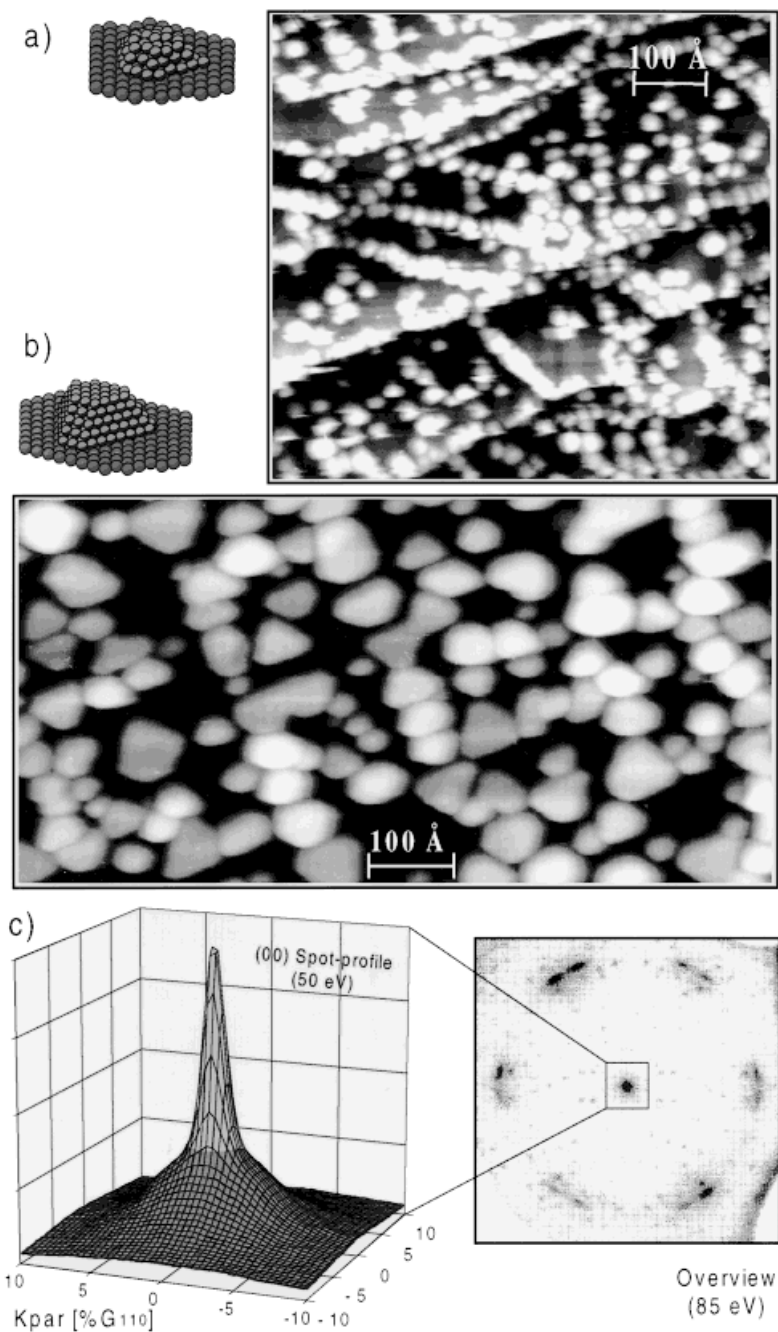


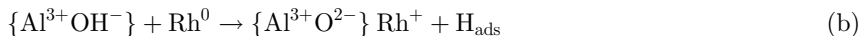
Fig. 6. Pd growth on  $\text{Al}_2\text{O}_3/\text{NiAl}(110)$ : a) STM image after Pd deposition at 90 K (CCT, +1.6 V, 2.2 nA). b) STM image after Pd deposition at 300 K (CCT, +0.4 V, 0.5 nA). c) LEED pattern after deposition of 20 Å Pd at 300 K (right hand side) and intensity profile of an area close to (00)-spot (left hand side)

However, it is not just a question of the existence of defects per se but also their nature. Palladium, for example, has a growth behavior that is influenced by the existence of domain boundaries, as well as by the steps of the substrate and point defects in the oxide layer (BÄUMER 1995). This is illustrated in Fig. 6a, in which Pd was deposited at 90 K.

The Pd particles partly decorate the domain interfaces, as can be seen in the figures. In addition, there are particles on the terraces. If the same amount of Pd is deposited at room temperature, the mobility is increased and clearly larger aggregates form. Some of the aggregates in Fig. 6b adopt the shape of small crystals. That these crystals are limited by planes with a (111) orientation is apparent from the electron diffraction diagrams, such as that shown in Fig. 6c (BÄUMER 1995). The oxide reflections are two diffuse, but clearly definable, hexagonal (111) superstructure reflections rotated 12° towards each other. The double reflections stem from the growth of the particles on both of the Al<sub>2</sub>O<sub>3</sub> domains. Recently, we have studied some aspects of the internal structure of the aggregates. Using transmission electron microscopy, it has been found that the average lattice constant of the aggregates decreases as a function of decreasing aggregate size. The magnitude of the effect depends on the particular metal and varies between 3–8% with respect to the bulk lattice constant (KLIMENKOW 1997, NEPIJKO 1 and 2). Also, it has been possible to atomically resolve terraces of some aggregates but imaging the entire island including the atoms at the oxide metal interface is still difficult (HANSEN).

Rhodium which is an important component in car exhaust catalysts exhibits a slightly stronger interaction with the substrate as compared with Pd. In the middle panel on the left of Fig. 5 rhodium has been deposited at room temperature on the clean alumina substrate. The mobility of rhodium at this temperature is such that the aggregates nucleate at the defects without coalescence due to the particular epitaxial growth conditions forming strings of deposited aggregates. In order to grow aggregates in a random distribution across the surface one could expose the surface at lower temperature as shown in Fig. 7 or hydroxylate the surface before exposure to the metal vapor (FRANK 1997).

If the latter is done, the impinging rhodium atoms chemically bind to the hydroxyl groups according to the reaction scheme



and this stabilizes smaller aggregate sizes at random distribution even at room temperature, as shown in Fig. 8. Once the aggregates have been formed and have reached a given size, they are stable over a considerable region of temperatures.

For example, the distribution of aggregates created by deposition at low temperatures (90 K), shown in Fig. 7, is morphologically stable up to 700 K. The rhodium aggregates prepared on the hydroxylated surface (Fig. 8) are even more stable. We may use the region of thermal stability of the aggregates to investigate chemical reactivities of such an ensemble of aggregates without changing morphologies. This brings us in a position to study a particular chemical reaction for a given particle size under very well defined conditions and proceed a step towards bridging the materials gap (FREUND 1997-1). Furthermore, if we are able to control the size of the deposited aggregates, then we should be in a position to explore the size dependence of chemical reactions in such systems. In catalytic reactions particle size selectivity of reactions has been used to

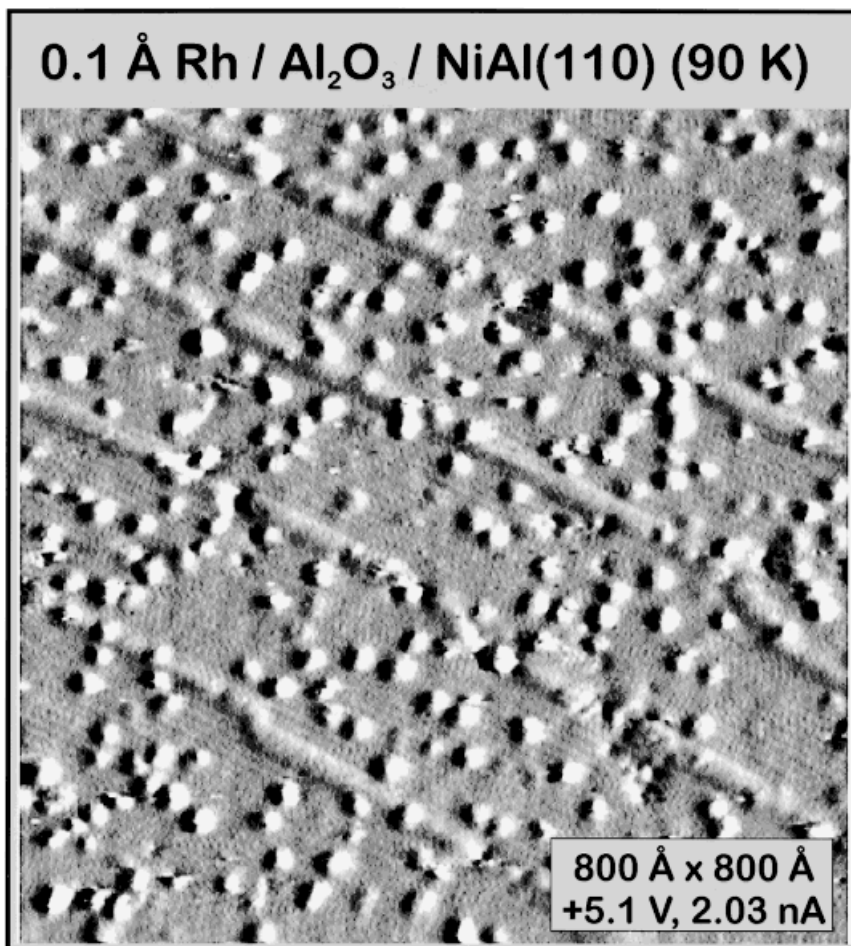


Fig. 7. STM image of 1/20 monolayer of rhodium deposited at 90 K onto an alumina model substrate. The light protrusions represent the deposited metal aggregates. The structure of the oxidic support is represented by the finer structure and the broad linear features are due to the antiphase domain defect structure at the surface

steer these reactions to certain products. CO dissociation has to be considered as one reaction channel in connection with automotive exhaust control, because it can lead to the deposition of carbon on the catalyst which in turn may poison its activity. We have chosen to investigate this very simple reaction, i.e. CO dissociation on rhodium aggregates. It is known from the study of the interaction of CO with rhodium aggregates deposited on alumina powders that CO shows a varying tendency to dissociate into carbon and oxygen atoms apparently depending on the size of the deposited rhodium aggregates. By varying particle sizes via the methods of nucleation and growth of metal particles on the alumina model substrate, we are now in a position to study the particle size dependence of this simple reaction in detail. The result of such a study is shown in Fig. 9.

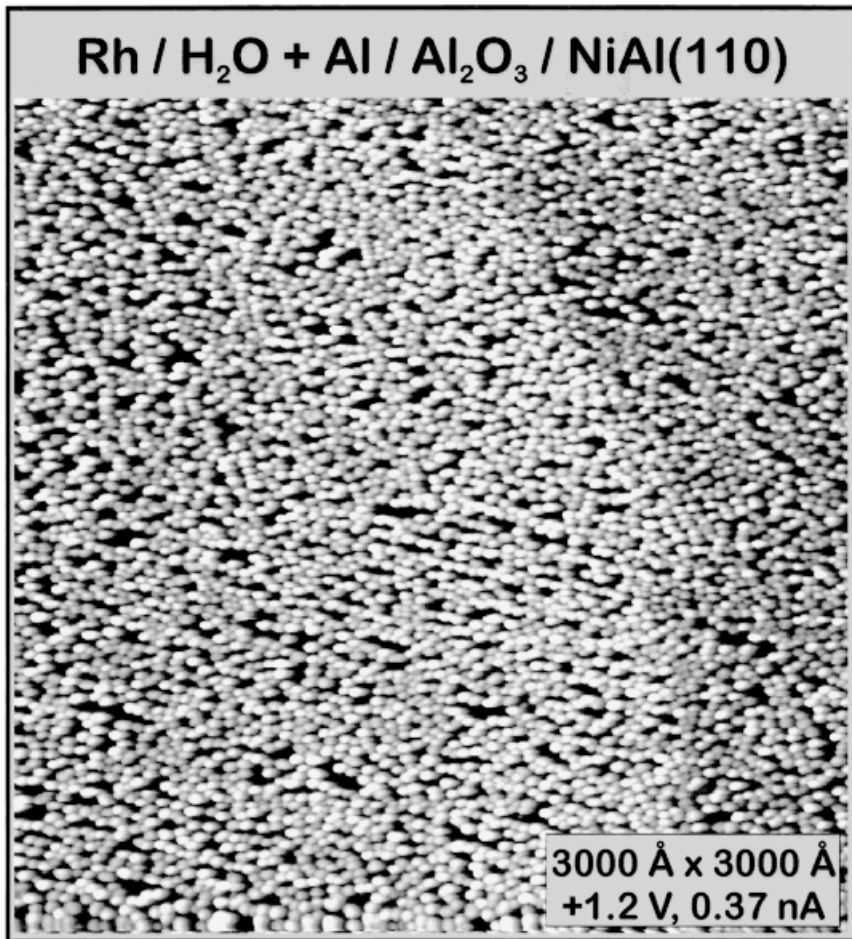


Fig. 8. STM image of rhodium deposited at room temperature onto a prehydroxylated alumina model substrate. In comparison with the rhodium deposit in Fig. 5 (which represents the non-hydroxylated surface) the distribution is considerably more uniform

The main result is the maximum in the dissociation rate observed for aggregates containing about 1000 atoms while for smaller as well as larger aggregates the dissociation rate is lower. It is well known for flat metal single crystal surfaces that CO does not dissociate upon adsorption but rather binds to the surface reversibly as a molecule. The introduction of steps on the surface is known to induce dissociation indicating that there are specific sites necessary for the dissociation reaction. A detailed analysis of the structure and morphology of the deposited aggregates as a function of size indicates that it is the creation and finally the diminution of steps that steers the reactivity. Again, resorting to Fig. 9 and following the dissociation rate curve from the left it has been shown that the smallest particles grow as two-dimensional layers and before the aggregates contain 100 atoms, the second layer starts to grow. Eventually, three dimensional particles grow but their height never exceeds their width. When the particles contain less than about 1000 atoms, the particles coalesce and the island density decreases consider-

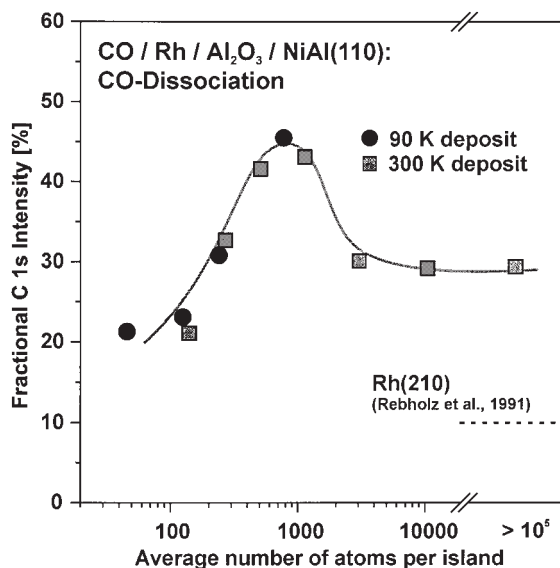


Fig. 9. Plot of the C1s intensity resulting from the dissociation of CO (adsorbed at 90 K, heated to 600 K) as a function of the average number of atoms per particle

ably. This is when the dissociation rate decreases and the maximum has been surpassed. Thus, it is quite easy to understand how the size-dependent reactivity comes about in this case. It turns out that the size of particles near 5 nm where we find highest dissociation rates indeed coincides with those sizes where high catalytic activities have been observed in various, also much more complex chemical reactions. Obviously, for a given metal/substrate combination certain particle sizes stabilize a maximum of active sites and thus maximizes the reaction rate. This, however, is only one ingredient in optimizing a catalytic reaction. Selectivity is another issue that has to be addressed in the future.

#### 4. Electronic structure and adsorption

Photoelectron spectra can be taken of the systems morphologically characterized in this way (SANDELL 1995, 1996 and 1998). With valence ionization as well as with ionization of inner shell electrons the dependency on the particle size can be established. We discuss for the clean adsorbate free particles only the inner ionization. Figure 10 summarizes for Pd deposits some 3d spectra, which were taken with synchrotron radiation.

The binding energy and the line width observed for the largest aggregates are practically the same as for the solid Pd(111) surface. One observes a clear shift to higher binding energies with decreasing particle size and at the same time a clear line broadening. Many effects could contribute to both of these observations (MASON 1983, WERTHEIM 1987 and 1989). Generally it can be said that charge transfer phenomena as well as so called initial state effects and also such influences which come about in the ionized state of the system could play a part. The discussion of line widths turns out to be especially difficult (MASON 1983, WERTHEIM 1987 and 1986, MARKS 1990, SCHÖNHAMMER 1977 and 1978). At the moment one can only suspect that the non equivalence of the different metal atoms within the differently sized aggregates and the

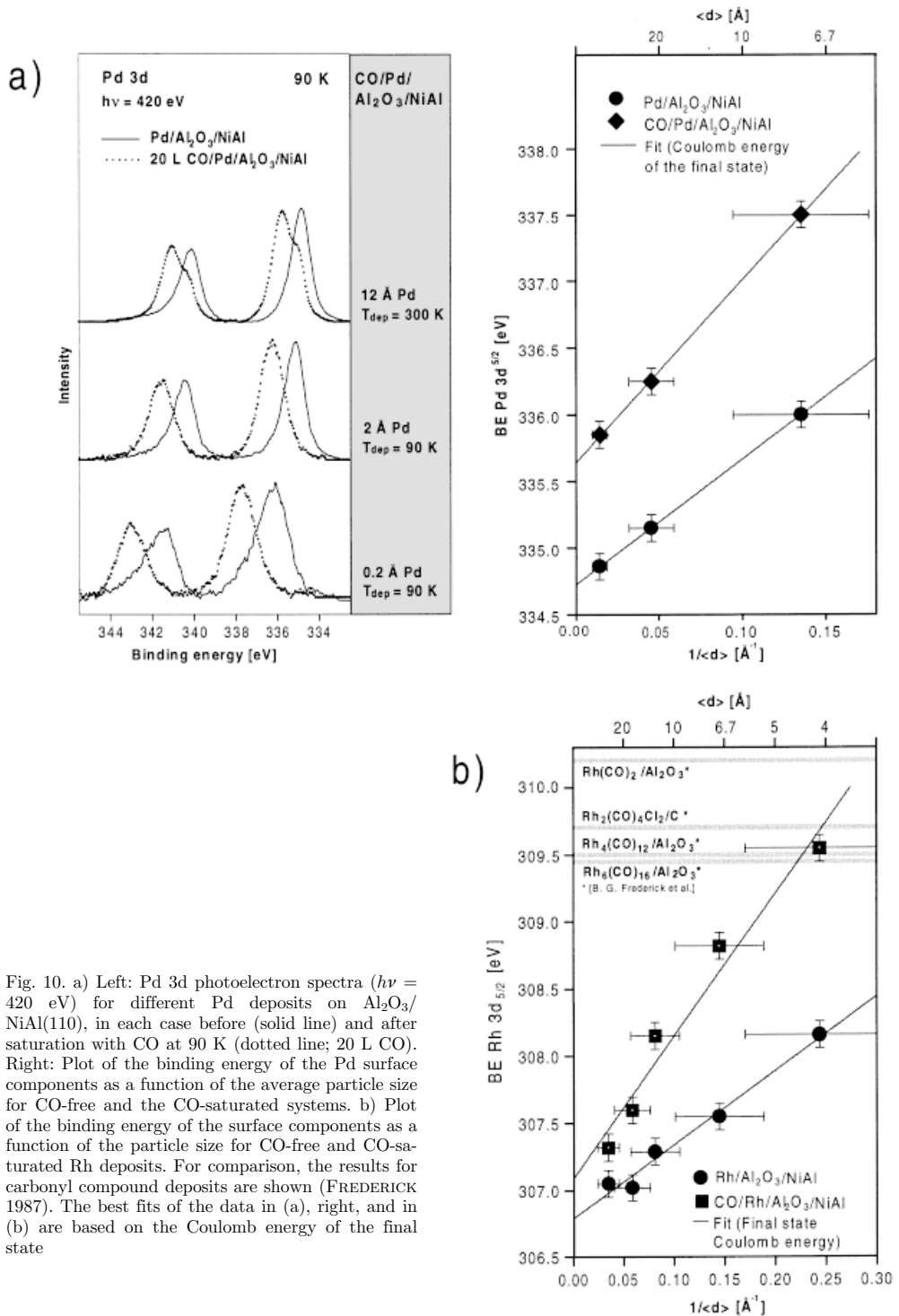


Fig. 10. a) Left: Pd 3d photoelectron spectra ( $h\nu = 420$  eV) for different Pd deposits on  $\text{Al}_2\text{O}_3/\text{NiAl}(110)$ , in each case before (solid line) and after saturation with CO at 90 K (dotted line; 20 L CO). Right: Plot of the binding energy of the Pd surface components as a function of the average particle size for CO-free and the CO-saturated systems. b) Plot of the binding energy of the surface components as a function of the particle size for CO-free and CO-saturated Rh deposits. For comparison, the results for carbonyl compound deposits are shown (FREDERICK 1987). The best fits of the data in (a), right, and in (b) are based on the Coulomb energy of the final state

interaction of a part of the metal atoms with the substrate combined with the final state effects are responsible for the spread.

In contrast, the interpretation of binding energy shifts which are graphically summarized on the right of Fig. 10a for Pd aggregates and in Fig. 10b for Rh aggregates turns out to be somewhat clearer (WERTHEIM 1989, DiCENZO 1985). Specific metal/support interactions (SCHÖNHAMMER 1977), in the sense, that charge is transferred from the metal to the support can be discussed using initial state effects. The discussion of final state effects is here also urgently necessary since the screening of the positive charge formed through ionization leads to clear binding energy shifts. Whilst for a bulk crystal a fully delocalised positive charge results, the charge delocalisation is limited for a metal aggregate not centrally bound to the substrate. Then a charge distribution builds up on the particle, whose size depends in accordance with the average radius of the particle (WERTHEIM 1989, DiCENZO 1985)

$$E_c \propto R^{-1} \quad (c)$$

and the binding energy shifts to higher binding energies with smaller radii. There is a number of experimental results (WERTHEIM 1986, 1987 and 1989, MARKS 1990, SCHÖNHAMMER 1977 and 1978, DiCENZO 1985) which are in accordance with equation (c) along with the explanation of the binding energy shift described in Fig. 10b. The shifts are put down fundamentally to final state effects. One would expect with a pronounced influence of charge transfer processes in a non ionized system a strong influence on the bonding energy of the substrate, which lies however in our case at 10% of the total effect. Possible reasons why pronounced charge transfer effects were observed with Pd (OGAWA 1995, SARAPATKA 1993-1 and -2) and Ni deposits on  $\text{Al}_2\text{O}_3$  layers which are on Al substrates, could be found for the different interactions on the metal/oxide interface depending on the defect density and stoichiometry of the film.

Binding energy shifts and line shapes change considerably if one adsorbs onto the metal deposits carbon monoxide. CO adsorption offers itself for study, because one has at one's disposal extensive comparative material of CO adsorption on metal single crystals (FREUND 1988 and 1997-2, KING 1990, MÅRTENSSON 1995). Figure 10 compares the Pd 3d spectra with and without CO coverage for desposits at 90 K and 300 K. If one looks at the available spectra after CO saturation at 90 K, the highest Pd coverage (corresponds to a mean island size of 70 Å) shows again clear similarities to the Pd(111) surface (ANDERSEN 1991 and 1994, BJÖRNEHOLM 1994). The Pd 3d signal of the clean surface shows a bulk and a surface component which are shifted towards one another by about 0.3 eV (FREUND 1988) and could not be resolved. CO adsorption leads to a shift of the surface component of ca. 1.1 eV to a higher binding energy whereby both sections (see shoulder in spectrum) could be well separated. The bulk portion amounts to 40% in this case, decreases to 13% with 2 Å Pd (average island size of 22 Å) and can no longer be distinguished at 0.2 Å Pd (average island size 7.5 Å). The comparison of the CO induced core level shifts shows that this grows with decreasing island size to ca. 1.5 eV. Experiments on single crystals show that the observed binding energy shifts depend on the number of coordinated CO molecules (ANDERSEN 1991, BJÖRNEHOLM 1994). Also a further analysis of the data (LIBUDA 1996-1) leads us to suspect that for smaller aggregates the number of coordinated CO molecules per surface Pd atom increases from one to two. The observed coordination numbers for transition metal carbonyls were never achieved (LIBUDA 1996-1). Nevertheless where one is able to compare the metal ioniza-

tion in carbonyl compounds with those from the deposited particles (FREDERICK 1987), the observed ionization energies from the carbonyl compounds with those of the smallest aggregate are in agreement. Figure 10b shows the comparison for Rh ionization. The obtained binding energies for the smallest aggregates are in agreement with the exact island sizes in the region of two to six nuclear metal carbonyls (FREDERICK 1987). The well known  $\text{Rh}(\text{CO})_2$  species on an  $\text{Al}_2\text{O}_3$  surface shows with 310.2 eV an even higher binding energy (FREDERICK 1987). Owing to the limited comparability of the substrate used, barriers are naturally set to such a comparison.

Further indications to the electronic structure of the systems can be derived from the valence as well as the C1s ionization of the adsorbed CO and also from thermal desorption spectroscopy (TDS). In Fig. 11 the TD-spectra of several Pd deposits are placed together (SANDELL 1996).

One finds with large Pd coverages a desorption spectrum which shows a large similarity to a spectrum of an adsorbate on a single crystal (GUO 1989). The relatively sharp, slightly intensive desorption maximum at 240 K stems from a hydrogen impurity (LIBUDA 1996-1). With decreasing size of the deposited particles comes a desorption maximum between 250 and 300 K. A possible objection regarding the comparability of the system prepared at 90 K with the films produced at higher growth temperatures refers to the fact that the thermal stability of the system is obviously limited. It is therefore fundamentally conceivable that the observed desorption between 200 and 300 K comes from a thermally limited structural reorganization of the metal aggregate alone due to the low growth temperature. A corresponding experiment based on the warming of the CO saturated systems to 300 K following a CO saturation at 90 K, shows however a virtually identical desorption spectrum (LIBUDA

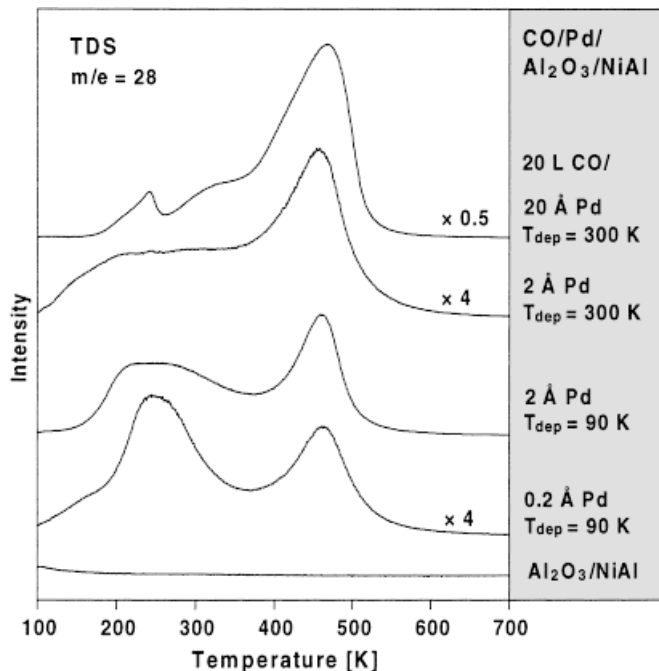


Fig. 11. TD spectra of CO ( $m/e = 28$ ) for the system CO adsorbed on Pd/ $\text{Al}_2\text{O}_3$ /NiAl(110) (20 L, adsorption temperature: 90 K, heating rate: about  $1.5 \text{ K s}^{-1}$ ). The sequence of the TD spectra corresponds to increasing particle size from bottom to top. The deposited amounts are given in terms of the effective layer thickness

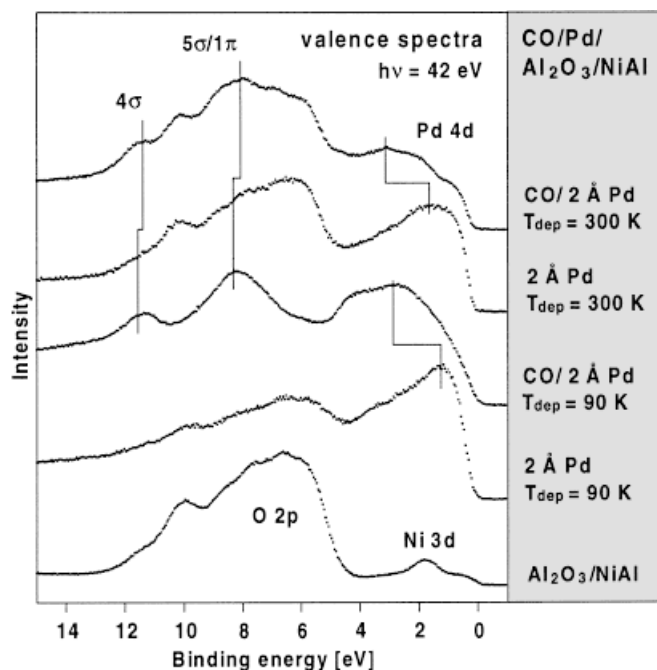


Fig. 12. Comparison of the valence photoelectron spectra of Pd deposited on  $\text{Al}_2\text{O}_3/\text{NiAl}$  before and after saturation with CO; ( $h\nu = 42 \text{ eV}$ )

1996-1). The low temperature desorption in the region of 200 to 300 K is an inherent property of very small Pd aggregates.

Figure 12 conveys the impression of the changes caused through CO adsorption in the region of the valence electrons (SANDELL 1996).

Firstly, one recognizes in the region of 11 eV and 8 eV binding energy the  $4\sigma$  or  $5\sigma/1\pi$  emission of the chemisorbed CO. The clearly higher intensity for the 90 K deposit in relation to the film prepared at room temperature is easy to understand with consideration of the growth behavior in the sense of a clearly larger surface area in the first case (LIBUDA 1996-1). The interaction of the valence states of the metal with the adsorbate leads to considerable changes in the region of Pd 4d emission. Also here the considerable difference in size of the aggregate shows clearly its dependence on the conditions of preparation: owing to the low proportion of bulk atoms at small coverages, CO saturation leads to even larger changes in the region of the Fermi level for the 90 K deposits.

The C1s spectra in Fig. 13 are typical for molecularly bound CO and therefore comparable to spectra of transition metal carbonyls (ANDERSEN 1991, BJÖRNEHOLM 1994, FREDERICK 1987) shown in the middle part of the figure and the C1s spectrum from CO adsorbed on Pd (111) shown above (ANDERSEN).

The weakly defined fine structure in the last shown spectrum is due to CO molecules on different adsorption sites. The C1s spectrum for 12 Å Pd is apart from an insignificant broadening identical to the spectrum of the single crystal adsorbate. By a transition to smaller aggregates one finds a significant shift to higher binding energies, an increase in the line width and an increase in the intensity of so called "shake-up" satellites (FREUND 1981-1, FUGGLE 1978, SCHÖNHAMMER 1980, GUNNARSON 1978, UMBACH

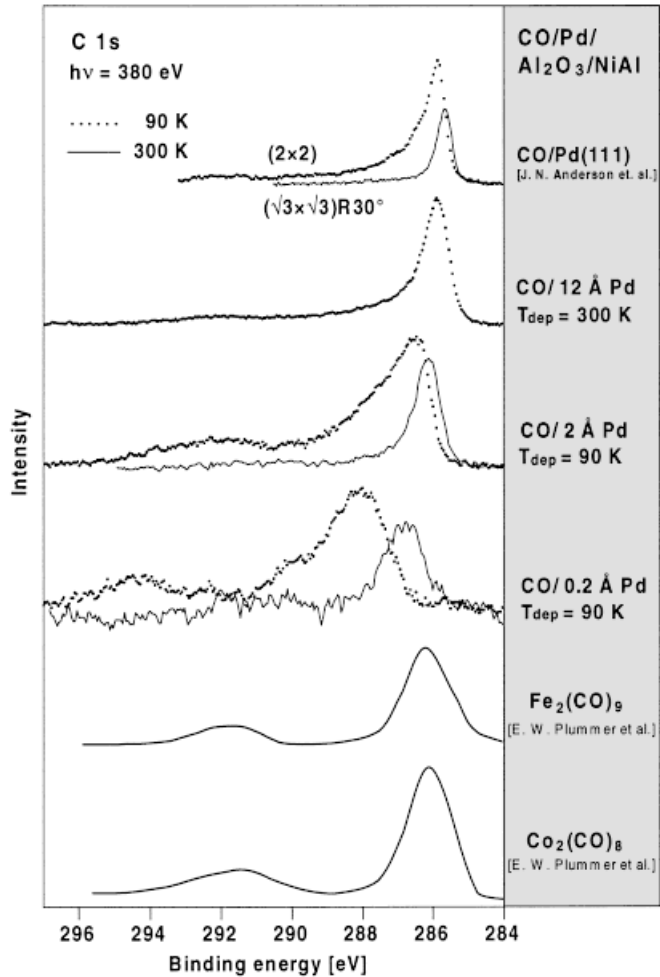


Fig. 13. C1s photoelectron spectra ( $h\nu = 380 \text{ eV}$ ) of CO/Pd/ $\text{Al}_2\text{O}_3$ /NiAl(110) after CO saturation at 90 K (dotted line) and after a short warming up to 300 K (solid line). For comparison, the C1s spectra of two ordered CO superstructures on Pd(111) (top) (ANDERSEN) as well as two transition metal carbonyls (bottom) are shown (PLUMMER 1978)

1982, NILSSON 1989, TILLBORG 1993, BAGUS 1981). After the removal of part of the CO through a short warming to 300 K a shift to lower binding energies as well as a decrease in line width, asymmetry and “shake-up” intensity is observed.

“Shake-up” satellites are one of the after discussed in the physics literature and well understood consequences of the fact that ionization is a complex many particle process and leads despite the emission of a single electron to the simultaneous excitation of many ion states (FREUND 1981-1, FUGGLE 1978, SCHÖNHAMMER 1980, GUNNARSON 1978, UMBACH 1982, NILSSON 1989, TILLBORG 1993, BAGUS 1981). How intensive these different ion states appear in the spectrum of an adsorbate depends on among other things, how strong the bond is between CO and metal (FREUND 1981-1 and -2, VON BARTH 1982). A detailed theoretical analysis shows that the charge transfer satellites in this respect have large intensities by a weak chemisorption coupling between CO and metal (FREUND 1981-1 and -2, BAGUS 1981). That means one may conclude, in agreement with the TDS experiments, from the change of the satellite intensities on an im-

portant change appearing with decreasing particle size: while the strength of the chemisorption bond sensitively depends for small aggregates on the coverage, this is not so much the case for large particles or single crystal surfaces. The lacking of well ordered crystal surfaces in the case of small aggregates leads inevitably to the situation that a distribution of different geometries must be taken into account and that these decisively contribute to the observed line broadening. Further effects can also contribute to the line width (TILLBORG 1993, NILSSON 1992-1) but shall not be discussed further here.

The observed binding energy shift must, as when dealing with the Pd ionization lead back to screening processes in the final state of the ionization (WERTHEIM 1989). In Fig. 14 compiled X-ray absorption experiments (LIBUDA 1996-1) verify this.

With the shown X-ray absorption the excitation is dealt with of a C1s or an O1s electron, respectively, into the unfilled  $2\pi$  orbital of the CO molecule (STÖHR 1991, VON BARTH 1982, NILSSON 1992-2 and 1995, BJÖRNEHOLM 1992). Since the excited electron in the  $2\pi$  orbital remains in the molecule, it takes care of a large part of the core hole screening. Whereas in the case of the C1s ionization the screening and with it the binding energy shift is strongly dependent on the particle size, one expects with X-ray absorption a much smaller influence from the particle size itself on the signal. Rather the strength of the bonding interaction between CO and metal influences the signal in the following way: the synergetic s-donor-p-acceptor bonding mechanism leads to an interaction between unfilled CO  $\pi$  orbitals and filled Pd 4d orbitals. Since the 4d orbitals form

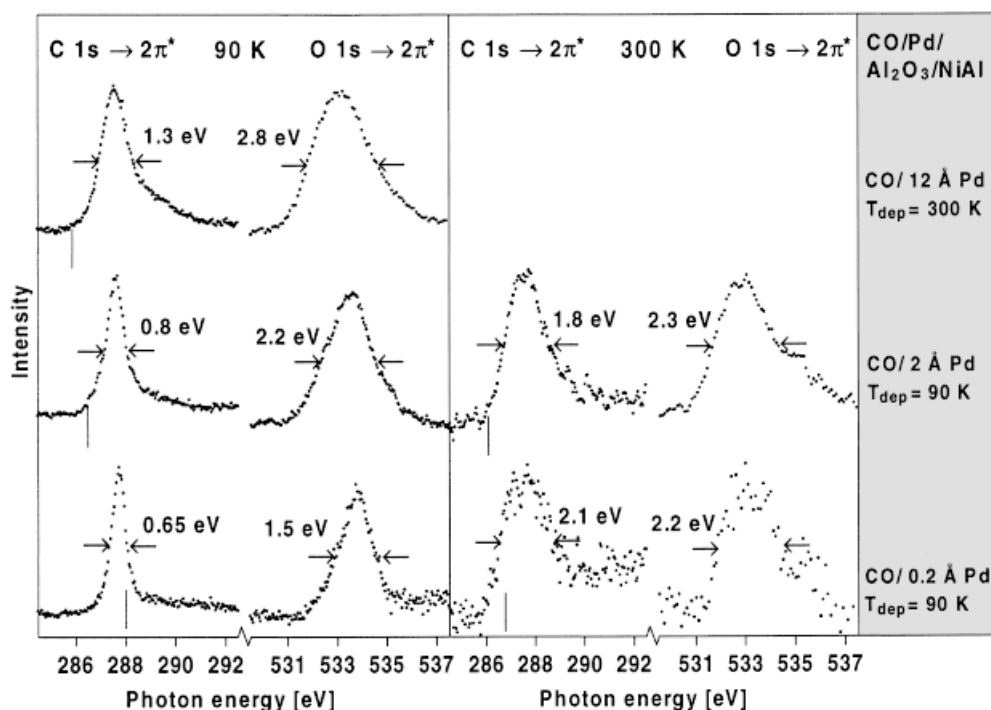


Fig. 14. X-ray absorption spectra of C1s and O1s  $\rightarrow \pi^*$  resonances for CO/Pd/Al<sub>2</sub>O<sub>3</sub>/NiAl(110). Left: After CO saturation at 90 K. Right: After short warming up to 300 K. The vertical marks show the position of the corresponding photoemission signals on a binding energy scale

a band, the interaction with the  $2\pi$  orbitals of the CO molecule leads to a  $2\pi$  state density distribution, whose width relative to the Pd 4d band width depends on the strength of the CO metal interaction. As systematic experiments on single crystal adsorption have shown, the lifetime of the excitation, vibrational excitations and intermolecular interactions play clearly a minimal role (BJÖRNEHOLM 1992). Two effects dominate: the width of the resonance increases for systems with the same geometry with increasing chemisorption energy, it also increases with increasing coordination of the CO molecule, that is by the transition from atop to bridge to hollow site. One can use these ideas for the interpretation of the resonance positions and widths in Fig. 14.

While the ionization energy shifts to larger values as a function of the decreasing particle size hinted at by the spike in the C1s  $\rightarrow$   $2\pi$ -spectrum, the C1s  $\rightarrow$   $2\pi$ -resonance stays more or less at the same energy. At the same time with larger aggregates it is broader as one expects by increasing chemisorption energy. The same is valid for the O1s  $\rightarrow$   $2\pi$ -resonance in the case of the deposition at 90 K. After heating to 300 K the resonance is wider in unison with the discussion conducted above. A clear indication of the strength of the bond! All experimental methods applied in complete agreement, point to a strong chemisorption bond in the region of small CO coverage for the Pd/Al<sub>2</sub>O<sub>3</sub> system for all island sizes. For small Pd aggregates the strength however decreases considerably for increasing coverage and lies finally for the smallest Pd aggregate and CO saturated coverage only in the region of weakly chemisorbed systems.

The comparison with Rh deposits is interesting here. Thermal desorption as well as X-ray absorption spectroscopy point to very much modest changes of the CO adsorption properties dependent on the aggregate size for Rh/Al<sub>2</sub>O<sub>3</sub>. Only the smallest islands show a slightly different desorption behavior. A possible explanation for the different behavior could lie in the differences of the smaller aggregates saturated CO adsorption geometry. It is known that Rh tends on the relevant adsorption sites to an overall higher coordination through the adsorbate in the sense of dicarbonyl species (GUO 1989). This is also in unison with the experiments not looked at in detail here (VAN'T BILK 1983, SOLYMOŠI 1985 and 1990, BASU 1987, ADEL T), which indicate a reconstruction of the Rh islands after CO exposure at 300 K, provable by corresponding LEED profile measurements, which lead after CO exposure at 90 K to an increased adsorption capacity (LIBUDA 1996-1).

The unique electronic properties of the deposited aggregates are also obvious from measurements where the aggregates are excited by electrons and the emitted light is spectroscopically collected (ADELT). The results of such cathode luminescence measurements are exemplified in Fig. 15 where a photograph of the experimental observation is shown together with two spectra recorded for two different average size distributions of deposited Pd aggregates.

The experimental set up is simple: The electrons are emitted from a cold field emitter tip and are accelerated towards the sample. The emitted light is collected via a spectrometer involving a l-N<sub>2</sub> cooled CCD camera. The blue spot is the light emitted from the sample as observed by the naked eye. The spectra are complex and we refer to the literature for details. Briefly, they contain a section up to 2.6 eV luminescence energy that involves excitations in the oxide/alloy substrate and another part between 2.6 and 5 eV which corresponds to emission from the deposited particles. The observed emission maxima change in energy position and intensity as a function of average aggregate size. This documents the quantum confinement of the electrons within the deposited metal

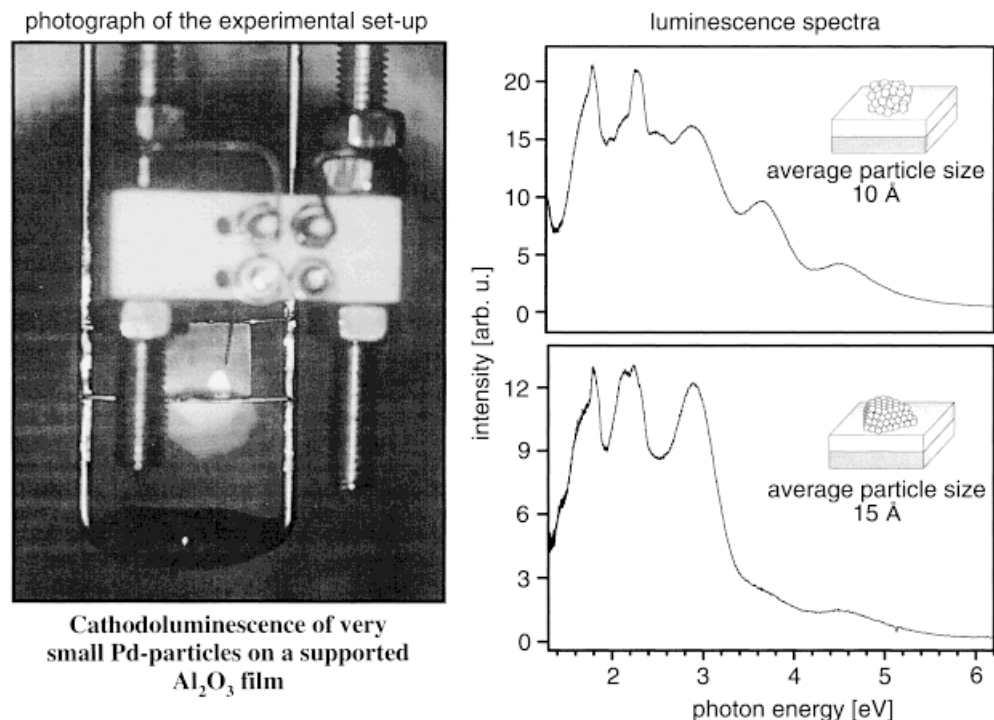


Fig. 15. The photograph shows the rectangular probe with a luminescent spot on its lower part. The ceramic holder of the field-emitter tip as well as the emitter wire can be seen. Two cathodoluminescence spectra are shown for clusters with an average size of 10 and 15 Å, respectively. The high energy bands are characteristic for such small particles while the bands at lower energy are also found for the pure substrate

aggregate as expected from a simple electron-in-a-box-approach. Detailed theoretical calculations have yet to be performed to allow for a final interpretation. One aspect is interesting with respect to a use of the light emitting properties of the aggregates, namely the expectation that these emissions could also be stimulated optically. This would allow us to probe the dynamics of electronic processes such as energy dissipation within the aggregate as a reaction is proceeding on the particle. We feel that the use of ultrafast lasers will help in the not too distant future to tackle some of these questions.

### 5. Adsorbate Vibrations

Vibrational spectroscopy is considered to be one of the most powerful tools to investigate the interaction of small metal aggregates with molecules adsorbed from the gas phase. We first discuss IR-studies for CO saturation on Pd aggregates (WOLTER 1998). Figure 16 contains corresponding data where on the left-hand side the Pd aggregates were grown at a substrate temperature near 90 K and on the right-hand side at a substrate temperature near 300 K.

The aggregates deposited at 300 K are crystalline with (111) facets parallel to the substrate. Such a situation can be described by aggregates of cubooctahedral symmetry (LAMBERT 1997, BÄUMER 1995).

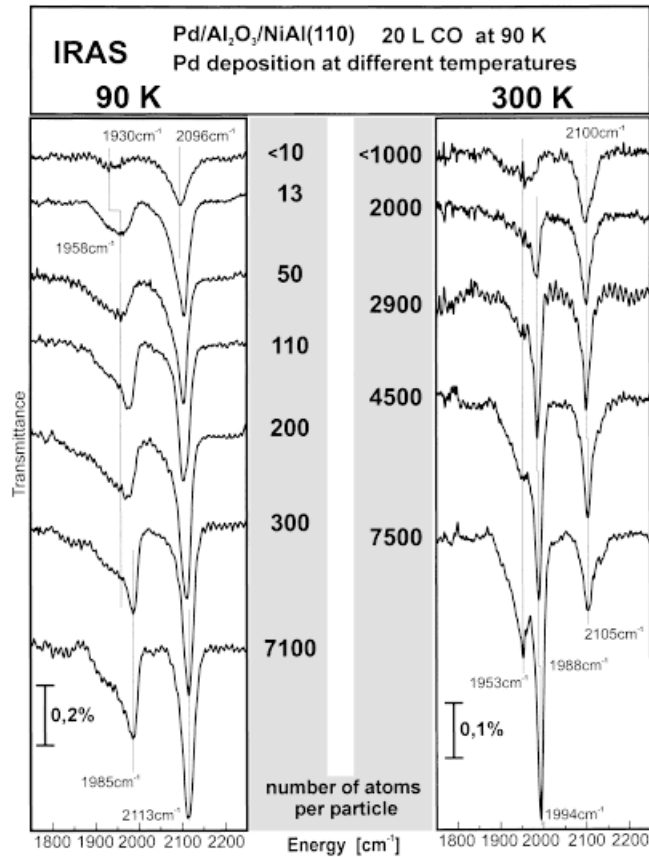


Fig. 16. Series of IR-spectra taken after deposition of different amounts of Pd at 90 K (left) and 300 K (right) and dosage of 20 L CO at 90 K. The average number of atoms per particle is given next to the spectra

We note from Fig. 17 that the amount of adsorbed CO as judged by the integrated CO signal intensity is considerably larger for the low temperature Pd deposits than for the room temperature deposits for a given amount of deposited metal. This is due to the larger surface area exposed by the irregularly shaped aggregates deposited at low temperature. As a general observation from Fig. 16 we realize that the positions of the bands for deposits at both temperatures are comparable. Furthermore, the line widths observed in Fig. 16 are, perhaps not unexpectedly, larger for the low temperature deposits due to the inherent higher degree of microscopic heterogeneity of Pd positions in those aggregates. It is possible to assign three regimes of frequencies for both sets of deposits based on the spectra for saturation coverage shown in Fig. 16. Those regimes are: 1930–1970 cm<sup>-1</sup>, 1970–2000 cm<sup>-1</sup> and 2090–2120 cm<sup>-1</sup>. On the basis of arguments presented below for the coverage dependent studies we assign these bands to bridge bonded species on the terraces of the aggregates (1930–1970 cm<sup>-1</sup>), to bridge bonded species on the edges of the aggregates (1970–2000 cm<sup>-1</sup>), and to terminally bonded CO (2090–2120 cm<sup>-1</sup>) not necessarily situated on the terraces, of course. The bands that we assign to CO bridge bonded on the edges of the aggregates have previously been assigned to CO on Pd(100) sites (BADRI 1992, RAINER 1996, EVANS 1996, TŪSHAUS 1990-1 and -2, KUHN 1992). The intensity of the absorption band in this region together

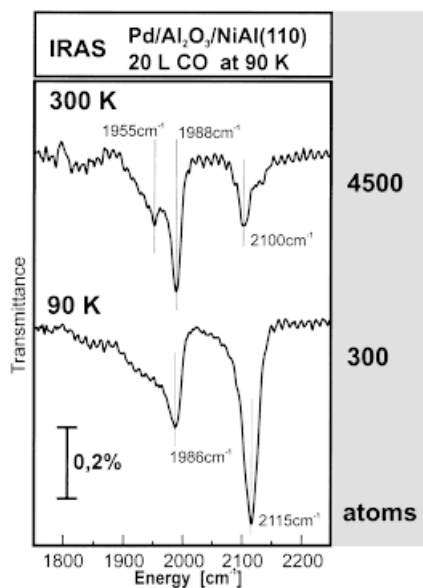


Fig. 17. Spectra for 4.4 Å Pd (average thickness) deposited at 300 and 90 K and a dosage of 20 L CO at 90 K

with the results from earlier SPA-LEED and STM-studies (FREUND 1997-1, BÄUMER 1995) lead us to a different interpretation (see below).

For the low temperature deposits there is a clear trend if we compare the intensity in the region of bridge bonded species with the intensity in the region of terminally bonded species as a function of aggregate size (Fig. 18, top). It is found that the fraction of bridge bonded species increases rapidly with the size of the aggregates until it reaches a saturation value. This is consistent with an increase of sites with two Pd atoms at the proper distance to be bridge bonded by CO molecules. If we compare this with the situation for the room temperature deposits also plotted in Fig. 18 (bottom), we realize the much slower increase starting from a higher level. Clearly, this is caused by the higher degree of order for the room temperature deposit already at the lowest metal coverage where the particles expose small terraces with atomic arrangements allowing for a considerable number of bridge bonds to be formed. Once the aggregates have assumed their regular shape, the relative ratio of bridge bonds to terminal bonds is only expected to change slowly (LAMBERT 1997, BÄUMER 1995). On the other hand, Pd(111) terraces bind CO molecules in a terminal geometry only at very high CO coverages ( $\theta > 0.7$ ) (LIBUDA 1994-2). On Pd(111) the terminally bonded CO with an adsorption band at about  $2100 \text{ cm}^{-1}$  is always accompanied by an intense band at about  $1900 \text{ cm}^{-1}$  which is assigned to a species adsorbed on threefold-hollow sites (TÜSHAUS 1990-2, KUHN 1992) (The shift of this band from about  $1830 \text{ cm}^{-1}$  at very low CO coverages is caused by dipole coupling (FERNANDEZ 1997)). At this high coverage the population of bridge sites is extremely low on Pd(111) (see above). The peak at about  $1900 \text{ cm}^{-1}$ , characteristic for CO molecules bound in threefold-hollow sites at high coverages, is not found in our spectra with corresponding large intensity but, if at all, as a weak shoulder. On Pd(111) for coverages of about  $\theta = 0.6-0.7$  the amount of terminally bonded CO is nearly zero and the CO is predominantly bridge bonded (see above) (BJÖRNEHOLM 1992). Combining all arguments the spectra indi-

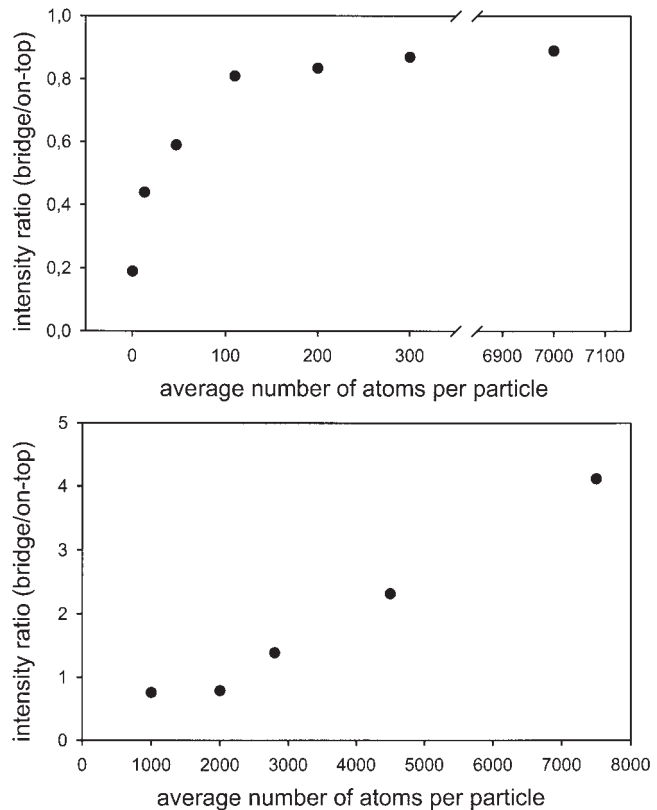


Fig. 18. Ratio of the integrated intensities of the absorption bands for bridge and on-top bonded CO for the 90 K (top) and the 300 K (bottom) deposits as a function of particle size

cate on one hand that on the facets of the Pd clusters the saturation coverage is smaller than saturation coverage ( $\theta = 0.75$ ) on a Pd(111) single crystal, and the CO molecules are preferentially bridge bonded on the aggregates. On the other hand, the above reasoning also explains why the intensity in the region of terminally bonded CO is considerably lower for the room temperature deposits, which exhibit well-ordered facets, i.e. because the coverage is below  $\theta = 0.75$ . In the spectral region assigned to the bridge bonded species there is a marked redistribution of intensity between the two sites, i.e. on the terraces and on the edges, favoring the edge bonded species for larger aggregates. This increase in intensity is too large to be understood on the basis of an increase in the number of sites (VAN HARDEVELD 1969) if we consider a cubooctahedron. We suggest here that it is due to dynamic intensity transfer via dipole coupling between the terrace bridge species with stretching frequencies at lower frequency towards the edge bridging species at higher frequency. Such an intensity transfer through dipole coupling would be consistent with what is known from single crystal surfaces (HOLLINS 1985 and 1992, PERSSON 1981). It is also consistent with the trend observed in Fig. 16 as the particle size increases. The larger the terraces grow and the more well-ordered the adsorbed CO islands are, the more pronounced the intensity transfer in the IR spectra becomes. After all the intensity transfer is a collective phenomenon depending on the size of the active domain (HOLLINS 1985 and 1992, PERSSON 1981).

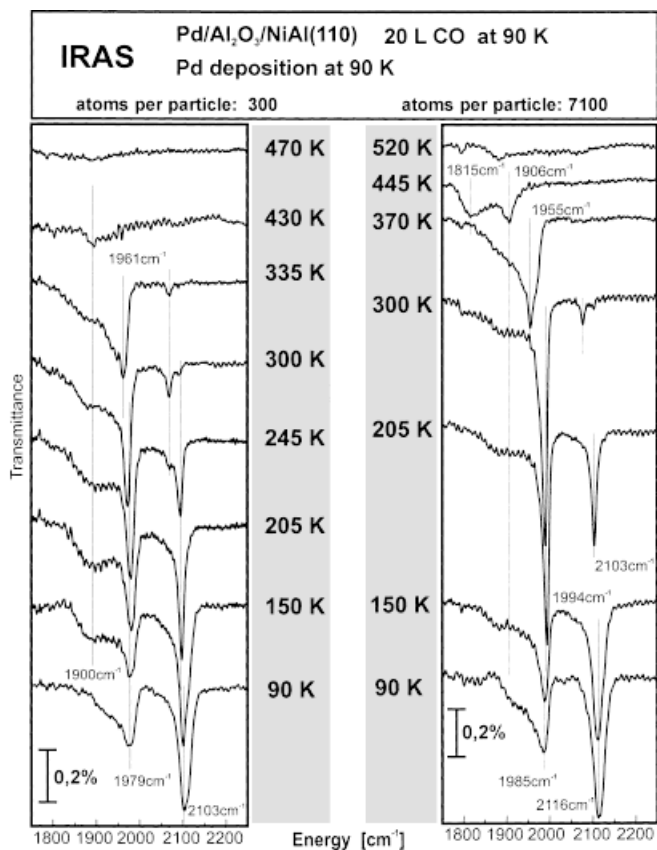


Fig. 19. IR-spectra for a lower (2.2 Å average thickness, left) and a higher (12 Å average thickness, right) Pd exposure at 90 K, dosage of 20 L CO and subsequent annealing to the indicated temperatures

As the next step we investigate the CO coverage dependence of the spectra (Fig. 19). We do this by starting at saturation coverage and subsequently heat the sample to the given temperatures. The spectra are then recorded again at 90 K. It is, of course, important for a consistent interpretation to keep in mind that upon heating above certain values the morphology of the aggregates may change. Figure 19 shows the coverage dependence for a smaller (i.e. 2.2 Å average thickness) and a larger (i.e. 12 Å average thickness) Pd exposure created at a substrate temperature of 90 K. The spectra for the highest coverage (lowest temperature) are similar to those reported in Fig. 16 and represent saturation coverage. We note the stronger relative population of bridge sites for the larger deposits. Upon decrease of coverage the peak in the area of terminally bonded CO (2090–2105  $\text{cm}^{-1}$ ) loses intensity and decreases in width until above room temperature the signal has almost completely disappeared. When the sample was heated (before recording the spectra at 90 K) above 200 K the band appeared to be split with a component located near 2070  $\text{cm}^{-1}$  growing in relative intensity. It is possible that this signal is due to isolated terminally bonded CO molecules (KÜNDIG 1972, GELIN 1984). As already discussed in connection with Fig. 16, the band due to bridge bonded species on the edges gains intensity before it undergoes a substantial transformation for the larger deposits. This transformation of band shape is more pronounced compared with the bands observed for the smaller amount of deposited material where changes are moderate.

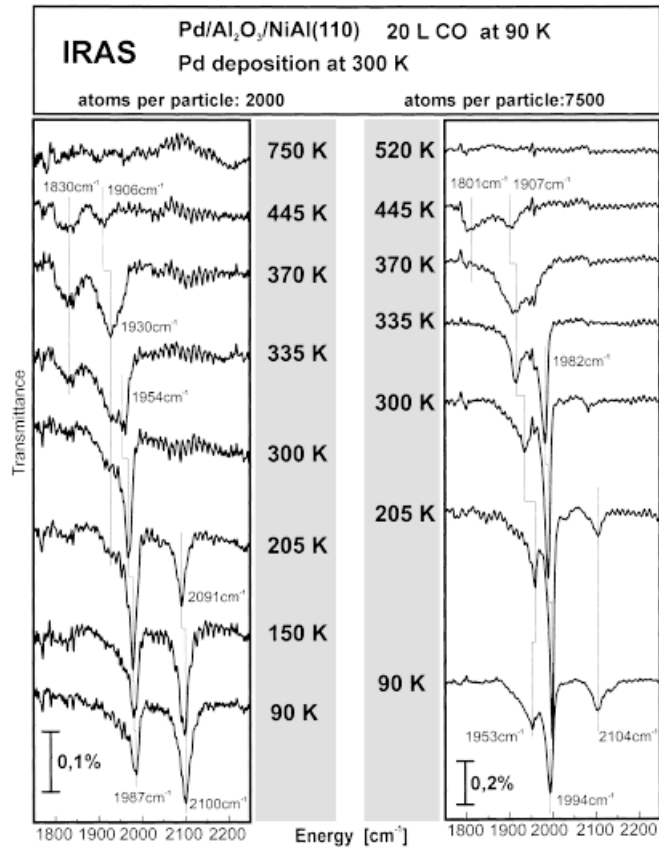


Fig. 20. IR-spectra of CO (20 L) adsorbed at 90 K on two different 300 K Pd deposits (average thickness: left: 1 Å; right: 12 Å). The systems were annealed to the temperatures given

To complement the discussion on the low temperature deposits again with corresponding data on the high temperature deposits, we show in Fig. 20 the coverage dependence for Pd deposited at 300 K.

On the left, a small amount of Pd (i.e. 1 Å average thickness) and on the right, a larger amount of Pd (i.e. 12 Å average thickness) has been evaporated onto the aluminum oxide substrate. In comparison with Fig. 19 the observed band widths are generally somewhat smaller and the frequencies are shifted but overall similar bands are found as discussed above. This is in particular true if only small amounts of Pd are deposited. The relative population of bands due to bridge bonded species is higher again but the coverage dependence up to an annealing temperature of 335 K is very similar to what has been observed for the low temperature Pd deposits. Above 335 K it is possible to completely desorb the bridging molecules on edges and to have only the bridging molecules on terraces as well as another species present. This extra species shows an absorption band near  $1830 \text{ cm}^{-1}$  and seems to be the most stable CO species on the aggregate. By comparison with data for low CO coverage on Pd(111) it must be assigned to adsorption in threefold-hollow sites, i.e. those sites which dominate adsorption on Pd(111) single crystal surfaces between small and half monolayer coverages (FERNANDEZ 1997).

For larger Pd deposits the situation at saturation coverage is different from the smaller Pd deposits. Due to the formation of more well-ordered facets and sufficiently low coverage (see above) the population of terminally bonded CO is very low. The bridge site region dominates the spectrum up to an annealing temperature of 370 K. Upon annealing to high temperature we also find population of threefold hollow sites, typical for the Pd(111) single crystal surfaces (KUHNS 1992, FERNANDEZ 1997). However, by comparing the present data with single crystal data of well-ordered surfaces it is obvious that there are very pronounced differences. The adsorption behaviour on the aggregates compares best with defect rich single crystal surfaces (LIBUDA 1996-2), i.e. spectra of a Pd(111) single crystal surface with a high density of defects also show an absorption band in the region of 1970–2000  $\text{cm}^{-1}$  (BJÖRNEHOLM 1992).

So far we have shown spectra recorded at low temperature. Figure 21 shows a set of spectra recorded for a small Pd deposit at 300 K, comparable to Fig. 20 but recorded at room temperature.

The on-top signal at 2064  $\text{cm}^{-1}$  is, not surprisingly (see above), very low. The bands in the bridging region are broader than at 90 K and the change after subsequent heating cycles resembles the one found in Fig. 18. We believe that the larger widths of the lines are due to the fact that the molecules are rather dynamic on the aggregate, i.e. other sites become accessible at elevated temperatures. We show these spectra because they compare well with those reported in the literature for small metal aggregates (GOYHENEX 1996). Those have also been assigned to bridge bonded species. Henry et al (GOYHENEX 1996) have published a similar spectrum for Pd deposited on MgO(100) where the aggregates also expose predominantly Pd(111) facets. However, Pd(111) and Pd(100) show similar spectra for saturation coverage at 300 K (BRADSHAW 1978) so that

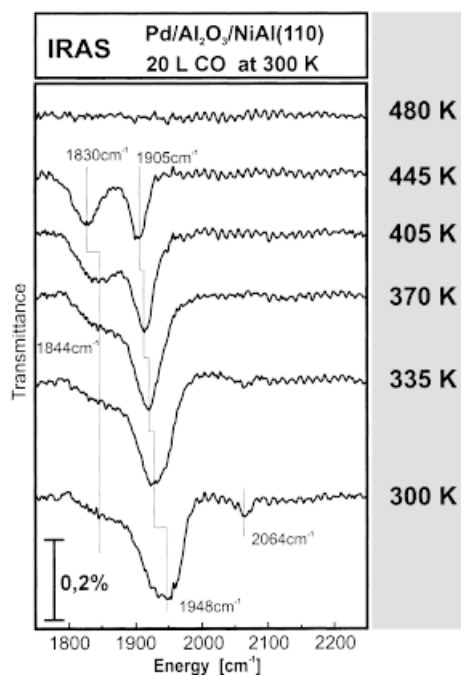


Fig. 21. Series of IR-spectra for 2.2 Å Pd (average thickness) deposited at 300 K, dosage of 20 L CO at 300 K and annealing to the given temperatures. All spectra were recorded at 300 K

a discrimination between the facets on the basis of the IRAS data recorded at 300 K is not really possible.

We have undertaken a corresponding study for Rh deposits on the clean as well as on the hydroxylated alumina surface. These results are fully comparable with those reported for the Pd aggregates. In addition, we also see the formation of geminal Rh-dicarbonyls, a species known from in-situ IR studies on real catalysts.

A final analysis has yet to be carried out, but the IR results so far available show that this technique will give us major insight into details of chemical processes on aggregates even though a straight forward deduction of adsorbate structure from an analysis of vibrational shifts may not always be possible.

## 6. Magnetic Properties

In addition to investigations on electronic properties it is interesting to develop tools which allow us to study magnetic properties. Bases upon the experience we have developed with using electronic spin resonance (ESR) on radicals adsorbed on single crystal surfaces (SCHLIENZ 1995, KATTER 1997, RISSE 1998) we have started measurements of the ferromagnetic resonance (FMR) (HILL 1 and 2). To this end we prepare either a bulk single crystal oxide surface or an epitaxial thin oxide film under ultrahigh vacuum conditions and grow the metal aggregates on it. Such a sample is brought into a microwave cavity and the FMR is recorded. The sample, which is attached to a manipulator may be oriented with respect to the external field, and therefore the orientation of the direction of the magnetization is accessible.

Figure 22 shows such a measurement for Co particles on  $\text{Al}_2\text{O}_3(0001)$ , deposited at room temperature.

An uniaxial orientation is found with a single minimum at orientation of the field parallel to the surface plane. This means that the magnetization is also oriented in this way (HILL 2).

A very similar behavior is found for iron as plotted in Fig. 22b. The smaller asymmetry is a property of the specific metal. While upon heating the behavior does not change for Co, it becomes more complex for iron (see Fig. 23) (HILL 3).

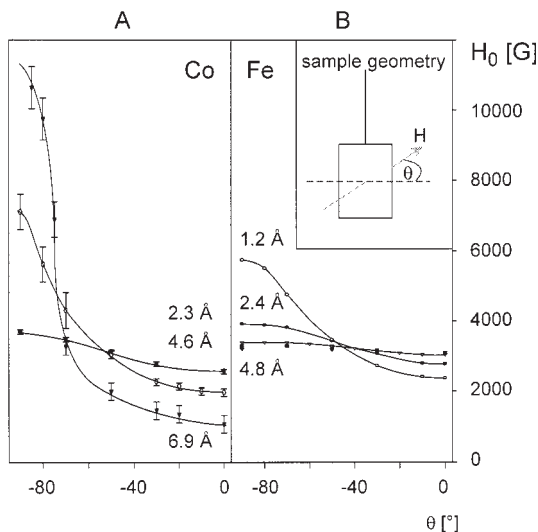


Fig. 22. Angular dependence of the resonance field for various amounts of Co and Fe deposited at room temperature on an  $\text{Al}_2\text{O}_3(0001)$ -single crystal surface.  $\theta$  denotes the angle between the crystal surface and the static magnetic field. The deposited amounts are given in terms of the effective layer thickness

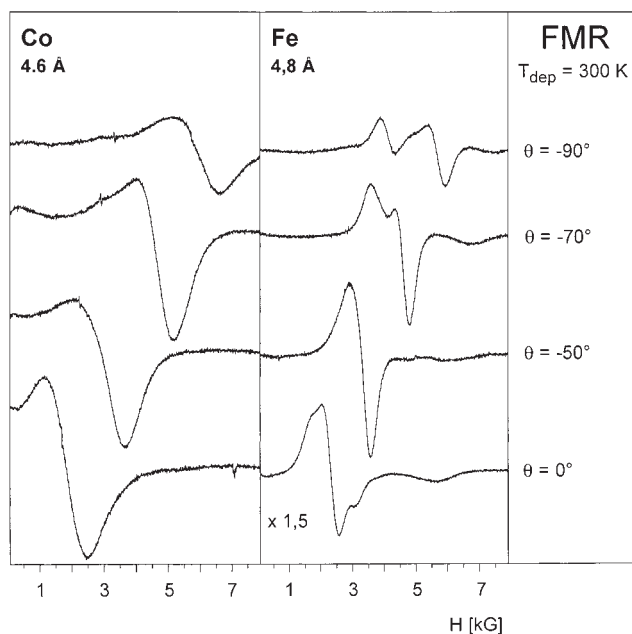


Fig. 23. Comparison of the angular dependent FMR-spectra of Co and Fe on  $\text{Al}_2\text{O}_3(0001)$  after heating the deposits prepared at 300 K to 870 K. The spectra were recorded at 300 K.  $\theta$  denotes the angle between the static magnetic field and the crystal surface. The deposited amounts are given in terms of the effective layer thickness

This is indicative for the survival of uniaxial magnetism in the hexagonal cobalt and its breakdown for the body centered cubic iron. Fe(bcc) has three easy axes of magnetization and the formation of more crystalline aggregates is likely to be the reason for the observation.

Since atomic resolution is very hard to achieve on the small aggregate at present, these experimental observations in the ferromagnetic resonance are very useful.

FMR can also be used to follow adsorption of the aggregates. We find that chemisorption of CO quenches the surface magnetism of the small particles. Oxidation of the small particles leads to the formation of an oxide skin on a ferromagnetic kernel. Since the oxide signal occurs at very different fields only the FMR of the kernel has been recorded. Such measurements may be used to follow the formation of oxide aggregates deposited on oxide supports which would have interesting catalytic properties.

## 7. Photochemistry

The small deposited aggregates lend themselves to photochemical studies, in which the influence of the aggregate size on the photochemistry on the surface of the particle is explored. In particular the photodesorption cross sections of small molecules such as NO from Pd aggregates have been studied (KAMPLING 1). In this case we heavily drew on our experience with photodesorption from oxide surfaces (AL-SHAMERY 1996). Very recently, photodesorption and photodissociation of methane from Pd aggregates of variable size has been investigated (KAMPLING 2). A gradual development of the chemistry towards the one observed on the compact single crystals is found. The smallest aggregates exhibit properties which are different from those expected for metals in line with some of the observations described for their electronic properties above.

*Acknowledgements*

We thank the *Deutsche Forschungsgemeinschaft*, *Bundesministerium für Bildung und Forschung*, and *Fonds der Chemischen Industrie* for support.

**References**

- ADAM, B.: Diploma Thesis, Ruhr-Universität Bochum 1991  
ADELT, M., NEPIJKO, S., DRACHSEL, W., FREUND, H.-J.: Chem. Phys. Lett., in press  
ALMY, D. B., FOYT, D. C., WHITE, J. M.: J. Electron Spectrosc. Relat. Phenom. **11** (1977) 129  
AL-SHAMERY, K.: Appl. Phys. A **36** (1996) 509  
ANDERSEN, J. N., QUARFORD, M., NYHOLM, R., SORENSEN, S. L., WIGREN, C.: Phys. Rev. Lett. **67** (1991) 2822  
ANDERSEN, J. N., HENNIG, D., LUNDGREN, E., METHFESSEL, M., NYHOLM, R., SCHEFFLER, M.: Phys. Rev. B **50** (1994) 7525  
ANDERSEN, J. N.: unpublished results  
BADRI, A., BINET, C., LAVALLEY, J.-C.: J. Chem. Soc. Faraday Trans. **92** (1992) 1603  
BAGUS, P. S., SEEL, M.: Phys. Rev. B **23** (1981) 2065  
BASU, P., PANAYOTOV, D., YATES Jr., J. T.: J. Phys. Chem. **91** (1987) 3133; J. Am. Chem. Soc. **110** (1988) 2074  
BAUER, E.: Zeitschrift für Kristallographie **110** (1958) 372  
BÄUMER, M., LIBUDA, J., SANDELL, A., WINKELMANN, F., FREUND, H.-J., GRAW, G., BERTRAMS, Th., NEDDERMEYER, H.: Ber. Bunsenges. Phys. Chem. **99** (1995) 1381  
BERTRAMS, Th., WINKELMANN, F., UTTICH, Th., FREUND, H.-J., NEDDERMEYER, H.: Surf. Sci. **331–333** (1995) 1515  
BJÖRNEHOLM, O., NILSSON, A., ZDANSKY, E. O. F., SANDELL, A., HERNNÄS, B., TILLBORG, H., ANDERSEN, J. N., MÅRTENSSON, N.: Phys. Rev. B **46** (1992) 10353  
BJÖRNEHOLM, O., NILSSON, A., TILLBORG, H., BENNICHT, P., SANDELL, A., HERNNÄS, B., PUGLIA, C., MÅRTENSSON, N.: Surf. Sci. **315** (1994) L983  
BRADSHAW, A. M., HOFFMANN, F. M.: Surf. Sci. **72** (1978) 513  
BUSTAD, J., ENKVIST, C., LUNELL, S., SVENSSON S.: J. Electron Spectrosc. Relat. Phenom. **70** (1995) 233  
CAMPBELL, C. T.: Surf. Sci. Rep. **27** (1997) 1  
CHATAIN, D., RIVOLLET, I., EUSTATHOPOULOS, N.: J. Chim. Phys. **83** (1986) 561, *ibid* **84** (1987) 201  
CHEN, J. G., CROWELL, J. E., YATES Jr., J. T.: J. Phys. Chem. **84** (1986) 5906  
CHEN, P. J., GOODMAN, D. W.: Surf. Sci. Lett. **318** (1994) L767  
COUSTET, V., JUPILLE, J.: Surf. Sci. **309** (1994) 309; Surf. Interface Anal. **22** (1994) 280  
DICENZO, S. B., WERTHEIM, G. K.: Comm. Solid State Phys. **11** (1985) 203  
EVANS, J., HAYDEN, B.E., LU, G.: Surf. Sci. **360** (1996) 61  
FERNANDEZ, V., GIESSEL, T., SCHAFF, O., SCHINDLER, K.-M., THEOBALD, A., HIRSCHMUGL, C. J., BAO, S., BRADSHAW, A. M., BADDELEY, C., LEE, A. F., LAMBERT, R. M., WOODRUFF, D. P., FRITZSCHE, V.: Z. Phys. Chem. **198** (1997) 73  
FRANK, M., ANDERSSON, S., LIBUDA, J., STEMPEL, S., SANDELL, A., BRENA, B., GIERTZ, A., BRÜHWILER, P. A., BÄUMER, M., MARTENSSON, N., FREUND, H.-J.: Chem. Phys. Lett. **279** (1997) 92  
FREDERICK, B. G., APAI, G., RHODIN, T. N.: J. Am. Chem. Soc. **109** (1987) 4797  
FREDERICK, B. G., APAI, G., RHODIN, T. N.: Surf. Sci. **244** (1991) 67  
FREUND, H.-J., PLUMMER, E. W.: Phys. Rev. B **23** (1981) 4859  
FREUND, H.-J., PLUMMER, E. W., SALANECK, W. R., BIGELOW, R. W.: J. Chem. Phys. **75** (1981) 4275  
FREUND, H.-J., NEUMANN, M.: Appl. Phys. A **47** (1988) 3  
FREUND, H.-J., DILLMANN, B., EHRLICH, D., HASSEL, M., JAEGER, R. M., KUHLENBECK, H., VENTRICE, C. A., WINKELMANN, F., WOHLRAB, S., XU, C., BERTRAMS, Th., BRODDE, A., NEDDERMEYER, H.: J. Mol. Catal. **82** (1993) 143  
FREUND, H.-J.: Angew. Chem. Int. Ed. Engl. **36** (1997) 452  
FREUND, H.-J.: Handbook of Heterogeneous Catalysis (Eds.: Ertl, G., Knözinger, H., Weitkamp, J.) Part A Chapter 5.1, Section 5.1.1 Principles of Chemisorption, 1997

- FUGGLE, J.C., UMBACH, E., MENZEL, D., BRUNDLE, K.: *Solid State Commun.* **27** (1978) 65
- GAYLORD, R. H.: PhD Thesis, University of Pennsylvania 1987
- GELIN, P., SIEDLE, A.R., YATES Jr., J.T.: *J. Phys. Chem.* **88** (1984) 2978
- GOYHENEX, C., CROCI, M., CLAEYS, C., HENRY, C. R.: *Surf. Sci.* **352–354** (1996) 475
- GUNNARSSON, O., SCHÖNHAMMER, K.: *Phys. Rev. Lett.* **41** (1978) 1608
- GUO, X., YATES Jr., J. T.: *J. Chem. Phys.* **90** (1989) 6761
- HANSEN, K. H., STEMPEL, S., BÄUMER, M., STENSGAARD, I., BESENBACHER, F., FREUND, H.-J.: unpublished
- HE, J. W., CORNELLE, J. S., ESTRADA, C. A., WU, M. C., GOODMAN, J. D. W.: *Vac. Sci. Technol. A* **10** (1992) 2248
- HEIDBERG, J., MEINE, D.: *Ber. Bunsenges. Phys. Chem.* **97** (1993) 211
- HENZLER, M., STOCK, A., BÖL, M.: in: *Adsorption on Ordered Surfaces of Ionic Solids and Thin Films*, (Eds.: Freund, H.-J., Umbach, E.), Springer Series in Surface Sciences **33**, Springer Verlag, Heidelberg, 1993
- HILL, Th., MOZAFFARI-AFSHAR, M., SCHMIDT, J., RISSE, T., STEMPEL, S., HEEMEIER, M., FREUND, H.-J.: *Chem. Phys. Lett.*, accepted
- HILL, Th., STEMPEL, S., RISSE, T., BÄUMER, M., FREUND, H.-J.: *J. Magn. Mag. Mater.*, submitted
- HILL, Th.: PhD Thesis, Ruhr-Universität Bochum, in preparation
- HOLLINS, P., PRITCHARD, J.: *Prog. Surf. Sci.* **19** (1985) 275
- HOLLINS, P.: *Surf. Sci. Rep.* **16** (1992) 51
- ISERN, H., CASTRO, G. R.: *Surf. Sci.* **211/212** (1989) 865
- JAEGER, R. M., KUHLENBECK, H., FREUND, H.-J., WUTTIG, M., HOFFMANN, W., FRANCHY, R., IBACH, H.: *Surf. Sci.* **259** (1991) 235
- JAEGER, R. M., HOMANN, K., KUHLENBECK, H., FREUND, H.-J.: *Chem. Phys. Lett.* **203** (1993) 41
- JAEGER, R. M., LIBUDA, J., BÄUMER, M., HOMANN, K., KUHLENBECK, H., FREUND, H.-J.: *J. Electron Spectrosc. Relat. Phenom.* **64/65** (1993) 217
- KAMPLING, M.: PhD Thesis, Freie Universität Berlin, in preparation
- KAMPLING, M., WATANABE, M., MATSUMOTO, Y., AL-SHAMERY, K., FREUND, H.-J.: to be published
- KATTER, U. J., SCHLIENZ, H., BECKENDORF, M., FREUND, H.-J.: *Ber. Bunsenges. Phys. Chem.* **97** (1993) 340
- KATTER, U. J., HILL, Th., RISSE, T., SCHLIENZ, H., BECKENDORF, M., KLÜNER, Th., HAMANN, H., FREUND, H.-J.: *J. Phys. Chem. B* **101** (1997) 552
- KING, D. A., WOODRUFF, D. P.: *The Chemical Physics of Solid Surfaces and Heterogeneous Catalysis*, **3**, Chemisorption Systems, Part A, Elsevier 1990
- KLIMENKOV, M., NEPIJKO, S. A., KUHLENBECK, H., BÄUMER, M., SCHLÖGL, R., FREUND, H.-J.: *Surf. Sci.* **391** (1997) 27
- KUHN, W. K., SZANYI, J., GOODMAN, D. W.: *Surf. Sci. Lett.* **274** (1992) L611
- KÜNDIG, E. P., MOSKOVITS, M., OZIN, G. A.: *Can. J. Chem.* **50** (1972) 3587
- LAMBERT, R. M., PACCHIONI, G. (Eds.): *Chemisorption and Reactivity on Supported Clusters and Thin Films*, NATO ASI Series, Series E, **331**, Kluwer, Dordrecht, 1997
- LIBUDA, J., BÄUMER, M., FREUND, H.-J.: *J. Vac. Sci. Technol. A* **12** (1994) 2259
- LIBUDA, J., WINKELMANN, F., BÄUMER, M., FREUND, H.-J., BERTRAMS, Th., NEDDERMEYER, H., MÜLLER, K.: *Surf. Sci.* **318** (1994) 61
- LIBUDA, J., SANDELL, A., BÄUMER, M., FREUND, H.-J.: *Chem. Phys. Lett.* **240** (1995) 429
- LIBUDA, J.: PhD Thesis, Ruhr-Universität Bochum 1996
- LIBUDA, J., FRANK, M., SANDELL, A., ANDERSSON, S., BRÜHWILER, P. A., BÄUMER, M., MARTENSSON, N., FREUND, H.-J., in: *Elementary Processes and Excitations and Reactions on Solid Surfaces*, Springer Series in Solid State Sciences, **121**, 1996, p. 210–216
- LIBUDA, J., FRANK, M., SANDELL, A., ANDERSSON, S., BRÜHWILER, P. A., BÄUMER, M., MARTENSSON, N., FREUND, H.-J.: *Surf. Sci.* **384** (1997) 106
- MARKS, F. A., LINDAU, I., BROWNING, R.: *J. Vac. Sci. Technol. A* **8** (1990) 3437
- MARTENSSON, N., NILSSON, A. in *Applications of Synchrotron Radiation*, Springer Series in Surface Sciences, Vol. **35**, (Ed.: Eberhardt, W.), Springer, Berlin 1995
- MASON, M. G.: *Phys. Rev. B* **27** (1983) 748
- MCDONALD, J. E., EBERHART, J. G.: *Trans. Met. Soc. AIME* **233** (1965) 512
- MUNDENAR, J. M.: PhD Thesis, University of Pennsylvania 1988

- NEPIJKO, S. A., KLIMENKOV, M., KUHLENBECK, H., ZEMLYANOV, D., HEREIN, D., SCHLÖGL, R., FREUND, H.-J.: Surf. Sci., in press
- NEPIJKO, S. A., KLIMENKOV, M., ADEL, M., KUHLENBECK, H., SCHLÖGL, R., FREUND, H.-J.: Langmuir, submitted
- NILSSON, A., MÅRTENSSON, N.: Phys. Rev. B **4** (1989) 10249
- NILSSON, A., MÅRTENSSON, N., SVENSSON, S., KARLSSON, L., NORDFORS, D., GELIUS, U., AGREN, H.: J. Chem. Phys. **96** (1992) 8770
- NILSSON, A., BJÖRNEHOLM, O., ZDANSKY, E. O. F., TILLBORG, H., MÅRTENSSON, N., ANDERSEN, J. N., NYHOLM, R.: Chem. Phys. Lett. **197** (1992) 12
- NILSSON, A., MÅRTENSSON, N.: Physica B **209** (1995) 19
- OGAWA, S., ICHIKAWA, S.: Phys. Rev. B **51** (1995) 17231
- PAUL, J., HOFFMANN, F. M.: J. Phys. Chem. **21** (1986) 5321
- PERSSON, B. N. J., RYBERG, R.: Phys. Rev. B **24** (1981) 6954
- PFNÜR, H., SCHWENNICKE, C., SCHIMMELPFENNIG, J., in: Adsorption on Ordered Surfaces of Ionic Solids and Thin Film, (Eds.: Freund, H.-J. and Umbach, E.), Springer Series in Surface Sciences, **33**, Springer Verlag, Heidelberg 1993, p. 124
- PLUMMER, E. W., SALANECK, W. R., MILLER, J. S.: Phys. Rev. B **18** (1978) 1673
- RAINER, D. R., WU, M.-C., MAHON, D. I., GOODMAN, D. W.: J. Vac. Sci. Technol. A **14** (1996) 1184
- REBHOLZ, M., PRINS, R., KRUSE, N.: Surf. Sci. Lett. **259** (1991) L797
- RISSE, T., HILL, Th., SCHMIDT, J., ABEND, G., HAMANN, H., FREUND, H.-J.: J. Chem. Phys. **108** (1998) 9615
- SANDELL, A., LIBUDA, J., BRÜHWILER, P., ANDERSSON, S., MAXWELL, A. J., BÄUMER, M., MÅRTENSSON, N., FREUND, H.-J.: J. Electron Spectrosc. Relat. Phenom. **76** (1995) 301
- SANDELL, A., LIBUDA, J., BÄUMER, M., FREUND, H.-J.: Surf. Sci. **346** (1996) 108
- SANDELL, A., LIBUDA, J., BRÜHWILER, P. A., ANDERSSON, S., BÄUMER, M., MAXWELL, A. J., MÅRTENSSON, N., FREUND, H.-J.: Phys. Rev. B **55** (1997) 7233
- SANDELL, A., LIBUDA, J., BRÜHWILER, P. A., ANDERSSON, S., BÄUMER, M., MAXWELL, A. J., MÅRTENSSON, N., FREUND, H.-J.: J. Vac. Sci. Technol. A **14** (1998) 1546
- SARAPATKA, T. J.: J. Phys. Chem. **97** (1993) 11274
- SARAPATKA, T. J.: Chem. Phys. Lett. **212** (1993) 37
- SCHILDBACH, M. A., HAMZA, A. V.: Surf. Sci. **282** (1993) 306
- SCHLIENZ, H., BECKENDORF, M., KATTER, U. J., RISSE, T., FREUND, H.-J.: Phys. Rev. Lett. **74** (1995) 761
- SCHÖNHAMMER, K., GUNNARSSON, O.: Solid State Commun. **23** (1977) 691
- SCHÖNHAMMER, K. S., GUNNARSSON, O.: Z. Phys. B **30** (1978) 297
- SCHÖNHAMMER, K., GUNNARSSON, O.: Phys. Scr. **21** (1980) 575
- SCHRÖDER, K. M., SCHÄFER, F., WOLLSCHLÄGER, J., HENZLER, M.: Surf. Sci. submitted
- SCHWENNICKE, C., SCHIMMELPFENNIG, J., PFNÜR, H.: Surf. Sci. **293** (1993) 57
- SOLYMOSSI, F., PASZTOR, M.: J. Phys. Chem. **89** (1985) 4789
- SOLYMOSSI, F., KNÖZINGER, H.: J. Chem. Soc., Faraday Transactions **8** (1990) 389
- STEMPEL, S.: PhD Thesis, Freie Universität Berlin, in preparation
- STÖHR, J.: NEXAFS Spectroscopy, Springer Series in Surface Sciences, Vol **25**, Springer, Heidelberg 1991
- TILLBORG, H., NILSSON, A., MÅRTENSSON, N.: J. Electron Spectrosc. Relat. Phenom. **62** (1993) 73
- TRUONG, C. M., WU, M. C., GOODMAN, D. W.: J. Am. Soc. **115** (1993) 3647.
- TÜSHAUS, M.: PhD Thesis, Berlin 1990.
- TÜSHAUS, M., BERNDT, W., CONRAD, H., BRADSHAW, A. M., PERSSON, B.: Appl. Phys. A **51** (1990) 91
- UMBACH, E.: Surf. Sci. **117** (1982) 482
- VAN HARDEVELD, R., HARTOG, F.: Surf. Sci. **15** (1969) 189
- VAN'T BILK, H. F. J., VAN ZON, J. B. A. D., HUIZINGA, T., VIS, J. C., KONINGSBERGER, D. C.: J. Phys. Chem. **87** (1983) 2264; J. Am. Chem. Soc. **107** (1985) 3139
- VESECKY, S. M., XU, X., GOODMAN, D. W.: J. Vac. Sci. Technol. A **12** (1994) 2114
- VON BARTH, U., GRASSMANN, G.: Phys. Rev. B **25** (1982) 5150
- WERTHEIM, G. K., DICENZO, S. B., BUCHANAN, D. N. E.: Phys. Rev. B **33** (1986) 5384
- WERTHEIM, G. K.: Z. Phys. **B66** (1987) 53

- WERTHEIM, G. K.: *Z. Phys.* **D12** (1989) 319
- WINKELMANN, F., WOHLRAB, S., LIBUDA, J., BÄUMER, M., CAPPUS, D., MENGES, M., AL-SHAMERY, K., KUHLENBECK, H., FREUND, H.-J.: *Surf. Sci.* **307–309** (1994) 148
- WOHLRAB, S., WINKELMANN, F., LIBUDA, J., BÄUMER, M., KUHLENBECK, H., FREUND, H.-J. in: *Surface Science Principles and Applications*, Eds. MacDonald, R.J., Taglauer, E.C., Wandelt, K., Springer, Berlin 1996, p. 193–202
- WOLTER, K., SEIFERTH, O., KUHLENBECK, H., BÄUMER, M., FREUND, H.-J.: *Surf. Sci.* **399** (1998) 190
- WU, M. C., ESTRADA, C. A., CORNEILLE, J. S., GOODMAN, D. W.: *J. Chem. Phys.* **6** (1992) 3892
- WU, M. C., TRUONG, C. M., GOODMAN, D. W.: *J. Phys. Chem.* **9** (1993) 4182
- WU, Y., TAO, H.-S., GARFUNKEL, E., MADEY, T. E., SHINN, N. D.: *Surf. Sci.* **336** (1995) 123
- WU, Y., GARFUNKEL, E., MADEY, T. E.: in preparation
- WUTTIG, M., HOFFMANN, W., JAEGER, R. M., KUHLENBECK, H., FREUND, H.-J.: *Mat. Res. Soc. Symp. Proc.* **221** (1991) 143
- ZECCHINA, A., SCARANO, D., BORDIGA, S., RICCHIARDI, G., SPOTO, G., GEOBALDO, F.: *Catal. Today* **27** (1996) 403

(Received June 15, 1998; Accepted July 3, 1998)

*Author's address:*

Prof. Dr. Hans-Joachim Freund  
Department of Chemical Physics  
Fritz Haber Institute of the Max Planck Society  
Faradayweg 4–6  
D-14195 Berlin, Germany